

Patterned communication between synthetic tissues and bacterial cells

Thomas Emil Caganek

Supervisor: Professor Hagan Bayley

Master of Science by Research in Chemical Biology

22nd August 2021

Department of Chemistry

New College, University of Oxford

Acknowledgments

I want to thank Professor Hagan Bayley for the opportunity to carry out research in his group and his insightful guidance throughout the project. I am thankful to Dr Ravinash Krishna Kumar who has guided and supported me in the lab. Ravinash was a mentor when it came to the scientific part of the project as well as the personal side of science. I also want to express my gratitude towards Matthew Cornall who has guided me through countless scientific obstacles and who has always helped to make our group a pleasant place to work. Additionally, I want to thank Linna Zou for her never-ending support during my MSc.

I am thankful to the other members of the Bayley group especially Jorin Riexinger & Zhong Hui Lim who have become great friends and made my time doing research unforgettable.

Lastly, I want to thank my dear friends Yutong Yin, Dan Patel & Francesca Smith who have helped me in countless scientific discussions and who have supported me on a personal level for many years.

Table of Contents

1 Introduction 6

1.1 Droplet interface bilayers & droplet networks 6

1.2 Interfacing synthetic cells with biological cells 8

1.3 The experimental setup and aim of the project 9

1.4 The biology behind localised gene expression 11

1.5 Droplet networks and bioimplantable devices 12

1.6 Overview of the project 13

2 Characterisation of the gene induction system & experimental setup 15

2.1. Introduction 15

2.1.1 Overview 15
2.1.2 Characterisation of gene induction by L-arabinose 15
2.1.3 Features of the L-arabinose operon that enable localised gene induction 17
2.1.4 Features of the experimental setup 17

2.2 Results and Discussion 18

2.2.1 Optimising growth and expression conditions of *E. coli* 18
2.2.2 Growth of the E. coli strain in defined and rich medium 20
2.2.3 mCherry induction in defined and rich medium 23
2.2.4 mCherry induction at varying L-arabinose concentrations 24
2.2.5 Forming a uniform agarose gel containing embedded *E. coli* cells 26
2.2.6 Optimising the gel thickness for imaging quality 28
2.2.7 The effect of a lipid-oil-solution on cell growth in a submerged hydrogel 29
2.2.8 Preventing dehydration of the hydrogel layer 30
2.2.9 mCherry induction under coincubation conditions 32

2.3 Summary 34

2.4 Materials & Methods 35

2.4.1 Bacterial strains 35
2.4.2 Preparation of bacterial media 35
2.4.3 L-arabinose responsive Plasmid 36
2.4.4 Preparation of the lipid/oil solution 36
2.4.5 Preparation of the bacteria-containing hydrogel layer 37
2.4.6 Image analysis 37

3 Gene induction using single droplets 38

3.1 Introduction 38

3.2 Results and Discussion 39

3.2.1 Controlling bilayer permeability with αHL 39
3.2.2 Optimising αHL insertion 41
3.2.3 Investigating droplet stability and contact angles in DHBs 44
3.2.4 Release of dyes into the hydrogel layer 48
3.2.5 Gene induction using single L-arabinose-containing droplets 51

3.3 Summary 56

3.4 Materials & Methods 58

3.4.1 DIB formation and dye diffusion experiments 58
3.4.2 The effect of oil phase composition on bilayer size and stability 58
3.4.3 Release of L-arabinose from single droplets 59

4 Patterned gene induction using printed droplet networks 60

4.1 Introduction 60

4.2 Results and Discussion 61

4.2.1 Introduction to the printing process 61
4.2.2 Constructing compact droplet networks in our experimental chamber 62
4.2.3 Investigating the structure of printed networks after an 18-hour incubation period 64
4.2.4 Localised induction of mCherry using droplet networks of varying volumes 66
4.2.5 Release of the inducer from the droplet network can be controlled by the protein pore αHL 71
4.2.6 A slow release of the inducer is required to activate gene expression in the bacterial strain 73
4.2.7 Localised gene induction requires the uptake and metabolism of the inducer by the bacterial cells 75
4.2.8 Balancing the release of the inducer from a network with its uptake by the bacterial cells 76
4.2.9 Patterned gene induction using droplet networks 79
4.2.10 Inducer release from patterned droplet networks must be balanced with inducer uptake to maintain high pattern fidelity 81

4.3 Summary 83

4.4 Materials & Methods 84

4.4.1 Assembly of droplet networks 84
4.4.2 Manual addition of L-arabinose 85
4.4.3 Imaging of the experimental chamber 85
4.4.4 Syto-9 experiments 85

5 Conclusion & Future Directions 86

5.1 Conclusion 86

5.2 Applications of the current system 87

5.2.1 Controlling the competition between two bacterial strains using droplet networks 87
5.2.2 Two-way communication between bacterial cells & droplet networks 88
5.2.3 Interfacing droplet networks with mammalian cells 90
5.2.4 Towards bioimplantable devices based on droplet networks 93

References 95

Abstract

Droplet networks (synthetic tissues) comprised of aqueous droplets interfaced by bilayers show great promise for the replacement and augmentation of native tissues. However, this requires droplet networks to interact with biological cells in a spatially precise manner. Here, we report the construction of 3D-printed synthetic tissues that locally control population gene expression in a layer of bacterial cells by the patterned release of a chemical inducer. Precise micron-sized areas of gene expression are achieved by controlling the rate of release of the inducer at a threshold concentration to match its subsequent uptake and consumption by the surrounding cells. Our system provides a basis for the construction of droplet networks capable of interacting with cells at a spatially precise level and serves as the groundwork for the use of synthetic tissues in medical applications requiring local control of native tissues.

1 Introduction

1.1 Droplet interface bilayers & droplet networks

Bottom-up synthetic biology aims to mimic biological cells and tissues from simple non-living building blocks to better understand and harness biological functions. In nature biological membranes provide a barrier that separates the cell from its surrounding. Uptake and release of molecules allows cells to tightly control the intracellular environment. Additionally, membranes serve as simple way of storing energy in the form of ion gradients (Watson, 2015).

When building more complex systems in synthetic biology, compartmentalisation becomes increasingly important to avoid unintended crosstalk between individual components (Kwok, 2010). Droplet interface bilayers (DIBs), that underlie the work in this thesis, are one of the most powerful technologies to build connected synthetic compartments.

When aqueous droplets (fL-μL in volume) are submerged into an oil phase containing dissolved lipid, a lipid monolayer will spontaneously form at the water-oil interface (Wallace et. al, 2008) (Fig. 1A). Droplets are mainly held together by dispersion forces. When an aqueous droplet is submerged into oil it exists at a local thermodynamic minimum. Lipophilic molecules tend to avoid contact with the aqueous solution. The resulting droplet shape minimizes this contact area. The hydrophilic part of the lipids will then surround the aqueous droplet. In experiments carried out in this work, the oil phase consists of a mixture of linear hydrocarbon chains such as undecane, and arylated silicone oil. A variety of lipids have been previously shown to form monolayers surrounding aqueous droplets: they range from

compositions emulating membranes of living organisms (Barlow et. al, 2017) to mixtures not commonly found in nature (A. Dupin & F.C. Simmel, 2019).

When two aqueous droplets, each surrounded by a monolayer of lipids, are brought into contact with each other, a lipid bilayer will form at the droplet-droplet interface (Fig. 1B), termed a droplet interface bilayer (DIB). A range of biological membrane proteins have been incorporated into DIBs ranging from protein pores such as α-hemolysin (αHL) to light-driven proton pumps such as bacteriorhodopsin (BR) (Bayley et. al, 2008).

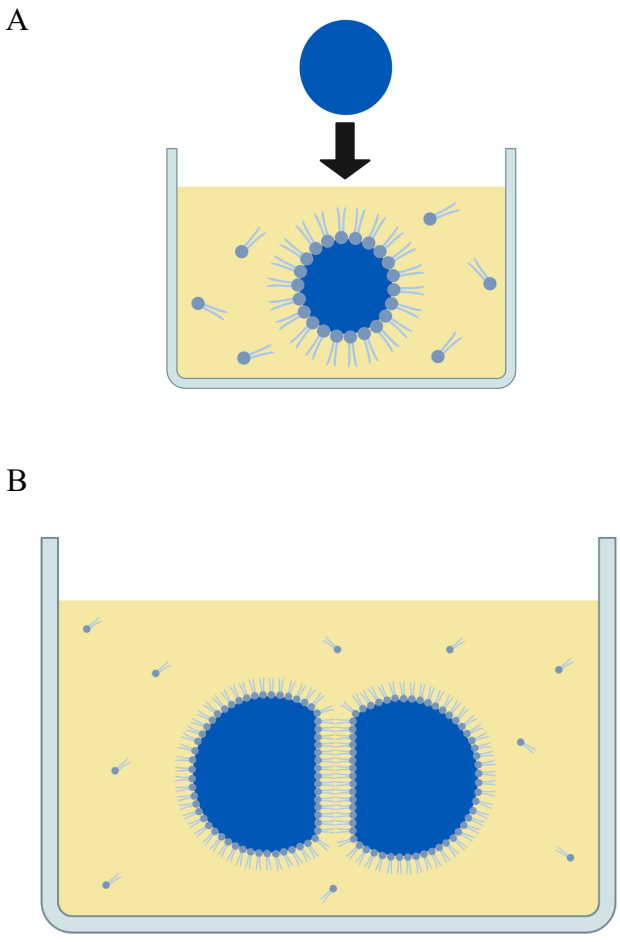


Figure 1.1: A diagram depicting (A) the formation of a lipid monolayer around an aqueous droplet submerged in an oil/lipid solution, and (B) the formation of a droplet interface bilayer when two droplets are brought into contact with one another.

Multiple droplets can be combined into larger structures to form droplet networks that have the potential to carry out more complex functions such as energy storage (Holden et. al, 2007), light sensing (Booth et. al, 2017) and computation of Boolean circuits (Yasuga et. al, 2016).

1.2 Interfacing synthetic cells with biological cells

Synthetic cells and tissues are systems made up of limited components that mimic their biological counterparts. Their limited complexity and potential to replicate biological functions make such systems ideal candidates for communication with biological systems. Interfacing biological cells with synthetic tissues could open up a broad range of new applications by enabling tight control of biological tissues. This has been the focus of several studies over the last years (Elani, 2020).

Synthetic cells have been shown to communicate with bacterial cells such as *Pseudomonas aeruginosa* by chemical means. Quorum sensing molecules can be produced by artificial cells and trigger a bioluminescence signal in the bacterial cell population (Rampiono et. al, 2018). Moreover, metabolites have been produced by vesicles that lead to an overproduction of a natural bioluminescence response in *V. harveyi* (Gardner et. al, 2009). More complex pathways of communication between biological and artificial cells have also been explored: artificial cells have been used as a translator by converting a chemical signal into an output that can then be sensed by bacterial cells (Lentini et. al, 2014) or allowing for the mediation of signals between different bacterial species (Lentini et. al, 2017). Chains of artificial cells have been used to trigger position-dependent activation of gene expression in bacterial cells by establishing morphogen gradients (Schwarz-Schilling et. al, 2016).

Lipid vesicles have been used for long term interactions between artificial cells and mammalian cells. The synthesis and slow release of a brain-derived neurotrophic factor in vesicles over several days can be used to drive differentiation and maturation in neural stem cells *in vitro* (Toparlak et. al, 2020).

Overall, past work in the field clearly shows the potential of artificial cells to impact native biological tissues. However, previous approaches lack spatial control over the interaction between artificial cells and biological tissues. Additionally, past work uses populations of single vesicles rather than spatially defined structures of interconnected compartments that could carry out more complex functions. Droplet networks could provide a solution to all of the above problems and could enable the construction of synthetic tissues that match the functionality of biological systems more closely.

1.3 The experimental setup and aim of the project

The aim of this project is to show that droplets and droplet networks are capable of locally inducing gene expression in a layer of bacterial cells. To achieve this, we grow bacterial cells in a thin hydrogel layer. The hydrogel layer is covered by a lipid/oil solution which leads to the formation of a monolayer at the droplet-gel interface. When an aqueous droplet is submerged, a bilayer forms between the droplet and the hydrogel, termed a droplet hydrogel bilayer (DHB) (Fig. 1.2). DHBs have been previously used in a different context to optically sense nucleic acids translocating through an αHL pore in the bilayer. A thin hydrogel layer is produced by spin coating to achieve thicknesses of below 300 nm (Leptihn et. al, 2013). Total internal microscopy (TIRF) is then used to detect changes in Ca^{2+} flux through the αHL pore caused by the translocation of DNA (Huang et. al, 2015).

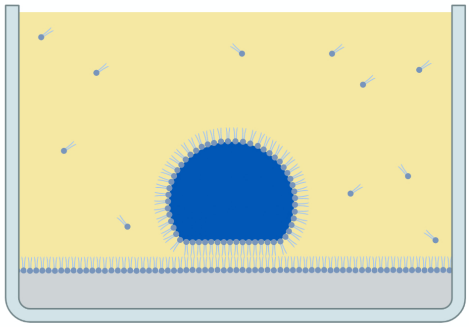


Figure 1.2: A diagram depicting the formation of a Droplet Hydrogel Bilayer (DHB). A hydrogel layer covers the bottom of the well and leads to the formation of a lipid monolayer at its interface with a lipid/oil solution. When an aqueous droplet is submerged in the well and comes into contact with the hydrogel, a bilayer will form at the droplet-hydrogel interface. Membrane proteins can then be inserted into the DHB.

In the experiments described in this work a layer of agarose covers the bottom of the well and contains a population of *Escherichia coli* (*E. coli)* cells modified with inducible genes under L-arabinose control. This layer is covered by an oil solution containing dissolved lipids. Aqueous droplets can then be submerged into the well and will form a bilayer between the aqueous droplets and the agarose layer. When aqueous droplets contain a protein pore (αHL) and a chemical inducer (L-arabinose), the inducer diffuses from the droplets into the gel layer and results in local activation of gene expression in the area of the gel that is exposed to a high concentration of inducer (i.e. directly below the droplet) (Fig. 1.3).

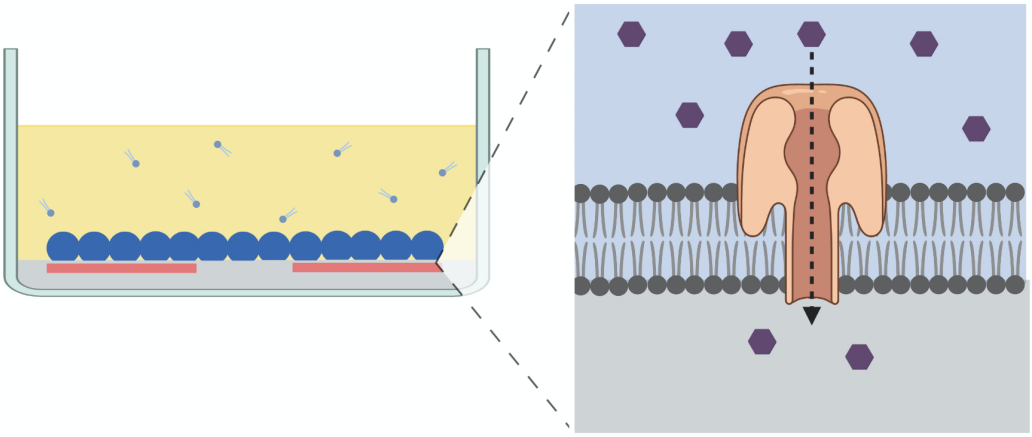


Figure 1.3: A diagram depicting the experimental setup used in this project. A droplet network containing an inducer and the protein pore αHL (shown in blue) is brought into contact with the bacteria-containing hydrogel (shown in grey). αHL inserts into the bilayer allowing for the diffusion of the inducer into the gel and its subsequent uptake by the bacterial cells leading to the expression of a fluorescent protein in that specific area (shown in red).

Our work shows that DHBs can be used to induce local changes in biological cells in close spatial proximity to droplet networks. Local changes in gene expression underlie many biological processes such as development or wound healing (Pastar et. al, 2014). Here, we chose gene induction in bacterial cells as a simple model system to illustrate the potential of using droplet networks to cause local changes in a population of biological cells.

1.4 The biology behind localised gene expression

The biological response in our model system is based on the L-arabinose-responsive P_{BAD} promoter. To achieve spatially localised induction of gene expression two main conditions must be met: 1) cells need to be exposed to a sufficiently high concentration of inducer for a sufficient period of time, 2) the inducer has to be

permanently consumed by the cells at a rate that prevents diffusion of the inducer away from its initial point of release (directly below the droplet network). If condition 1 is not met, no gene expression is observed. If condition 2 is not met the resulting gene expression pattern is diffuse and does not show localisation.

The arabinose-based system used here fulfils these criteria. Later chapters will examine several aspects of this system in more detail.

1.5 Droplet networks and bioimplantable devices

In large parts of this work, droplet networks consisting of hundreds of pL-sized droplets are used extensively over single aqueous droplets. Previous work in our group has shown the production of such synthetic tissues and the ability to functionalise these droplet networks to carry out cooperative behaviour such as folding (Villar et. al, 2013) (Fig. 1.4).

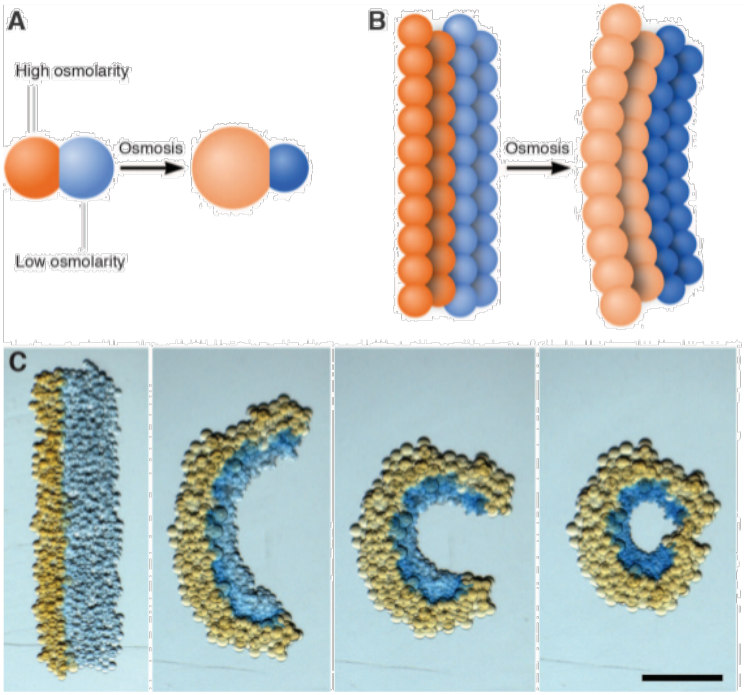


Figure 1.4: A depiction of self-folding droplet networks. Synthetic tissues containing several layers of droplets with different osmolarities lead to spontaneous folding of the structure. Scale bar = 200 μm. Adapted from (Villar et. al 2013).

Synthetic tissues provide a promising approach for the communication between artificial tissues and biological cells. In the past *in vitro* transcription and translation systems (IVTT) have been used to encode complex biological functions into synthetic tissues such as the production of a protein pore controlled by UV light (Booth et. al, 2016).

In the future we envision similar systems being used to sense and respond to damage and disease affecting native tissues in the body in a spatially controlled way. In the longer term, such bio-implantable devices could be used to augment and replace damaged organs and tissues.

1.6 Overview of the project

In the second chapter in this thesis, we examine the biology behind L-arabinose induction, optimisation of gene induction. The main challenge in this chapter is to find an experimental setup that allows for the coincubation of droplet networks and bacterial cells. This requires us to find conditions that are suitable for both bacterial cell growth and stable droplet networks. In the third chapter we explore droplet-hydrogel bilayer formation, insertion of the protein pore αHL into bilayers, diffusion of fluorescent molecules across bilayers, the droplet stability of single droplet systems and gene induction by releasing L-arabinose from single droplets. The main challenge in this chapter is to understand what factors influence to release of small molecules via a DHB with the use of αHL. In the fourth chapter we investigate the use of droplet networks as a way of interfacing aqueous droplets and biological cells. We explore the construction of droplet networks, the transfer of networks onto the

hydrogel layer, the stability of such structures over several hours, gene induction by releasing L-arabinose from droplet networks of varying volumes and patterns. The key challenge is to investigate whether a localised pattern of gene expression can be induced in a layer of bacterial cells using droplet networks and what conditions are required to achieve precise spatial control. The final chapter discusses future avenues of the work described herein.

2 Characterisation of the gene induction system & experimental setup

2.1. Introduction

2.1.1 Overview

Patterned gene induction in a homogenous population of *E. coli* cells using droplet networks requires cells that are able to respond to local inducer concentrations released from aqueous droplets. This chapter explores the biology and experimental setup behind this project. Firstly, we examined the growth *E. coli* in liquid and hydrogel conditions comprising of the rich undefined medium Lysogeny Broth (LB), or defined minimal medium (M9). Secondly, we investigated the conditions required to induce the production of a fluorescent protein under P_{BAD} control. Finally, we tested experimental setups that allow for the coincubation of the bacteria and the droplet-based systems.

2.1.2 Characterisation of gene induction by L-arabinose

The gene circuit used in the project is based on the inducible P_{BAD} expression system natively found in the L-arabinose operon in *E. coli*, our chassis of choice (Fig. 2.2). In our system, the fluorescent protein mCherry downstream of the P_{BAD} promoter is expressed in the presence of L-arabinose. L-arabinose is a monosaccharide that can be used a carbon source by bacterial cells. Sugar uptake is tightly controlled in *E. coli* by a mechanism called catabolite repression (Aidelberg et. al, 2014). A strict hierarchy of uptake exists with D-glucose being taken up first and yielding the highest growth rate (Ammar et. al, 2018). The L-arabinose operon ensures that L-arabinose is taken up only in the absence of the more favourable sugars D-glucose and L-lactose. In the presence of L-arabinose, a positive feedback loop is activated which

results in all-or-none induction. The expression of L-arabinose transporters encoded by the *AraE* gene are upregulated and result in an increased uptake of the monosaccharide. This further increases the intracellular L-arabinose concentration resulting in increased *AraE* expression (Khlebnikov et. al, 2000). The catabolic enzymes AraB, AraD and AraA break down L-arabinose via the pentose phosphate pathway (Fig. 2.1).

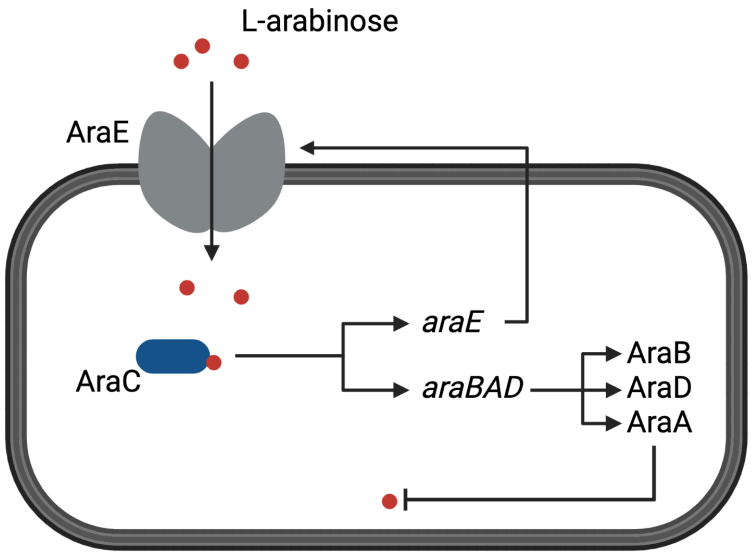


Figure 2.1: A diagram depicting the L-arabinose operon. L-arabinose is taken up by the *E. coli* cell via the AraE transporter. Inside the cells it binds to the transcription factor AraC leading to the upregulation of *araE* and *araBAD*. *araE* encodes the L-arabinose transporter resulting in more uptake of the inducer in a positive feedback loop. *araBAD* encodes the catabolic enzymes AraB, AraA and AraD that break down L-arabinose as a C-source.

2.1.3 Features of the L-arabinose operon that enable localised gene induction

There are two main reasons why we chose L-arabinose as the inducer in this project. Once inside the cell, L-arabinose is metabolised and is not released to the neighbouring cells. Additionally, L-arabinose shows very low permeability through the lipid membranes used in this work, which is essential for the controlled release of the inducer through αHL pores (A. Dupin & F.C. Simmel, 2019). These features allow us to match the release of the inducer from droplets to the rate at which it gets taken up and consumed by the bacterial cells. In this way no excess inducer can diffuse away from its original point of release and induce gene expression in undesired areas.

2.1.4 Features of the experimental setup

In the next part of this chapter, we characterised the experimental setup used in our work. To achieve the aim of the project, a layer of bacterial cells must be grown in conditions that allow for the placement of a droplet network in close proximity to those cells for several hours to allow for sufficient time for the induction of gene expression.

To achieve this, we investigated the use of agarose-based hydrogels as a basis for DHB systems. The release of small molecules can then be controlled by insertion of protein pores into this bilayer. Cells must therefore be able to grow and respond to the presence of the inducer while being covered by a lipid/oil solution. Additionally, we investigate methods for forming a flat hydrogel layer. This is important to ensure that there are not any surface irregularities that could potentially distort the droplet network sitting on top of the hydrogel layer. We also optimised the thickness of the hydrogel to allow for imaging of the cells and the droplet network. To achieve this the hydrogel must remain relatively thin (~200 μm-range). Furthermore, we investigated how to prevent dehydration of the hydrogel during the 18-hour timeframe of the

experiment to ensure that the gel layer does not shrink and tear. This is achieved by controlling the humidity during the incubation period.

2.2 Results and Discussion

2.2.1 Optimising growth and expression conditions of *E. coli*

In a first step we transformed the construct depicted in Fig. 2.2 into the *E. coli* strain BZB1011 *sfgfp*::*Tn7*. This strain contained genomically integrated super folded Green Fluorescent Protein (sfGFP) that was constitutively expressed (see methods). The plasmid used in this project contained 4797 base-pairs and expressed the red fluorescent protein mCherry in response to the inducer L-arabinose.

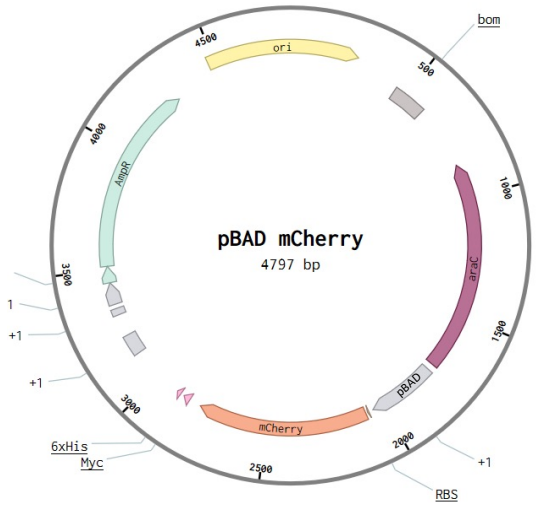


Figure 2.2: A diagram depicting the layout of the gene construct containing mCherry under the control of the P_{BAD} promoter.

After the initial transformation we examined the mCherry induction by growing the cells in liquid culture for 18 hours with 0.5% w/v (33 mM) L-arabinose. After overnight

growth the cells where imaged under an epifluorescence microscope. sfGFP was expressed in the presence (Fig. 2.3 A) and absence (Fig. 2.3 C) of the inducer, showing the expected constitutive expression of the genomically integrated fluorescent protein. mCherry was expressed in the presence of L-arabinose (Fig. 2.3 D) but not in its absence (Fig. 2.3 B). These results suggest that the gene construct responded to the presence of the inducer in liquid culture while showing minimal leakage of mCherry in these conditions.

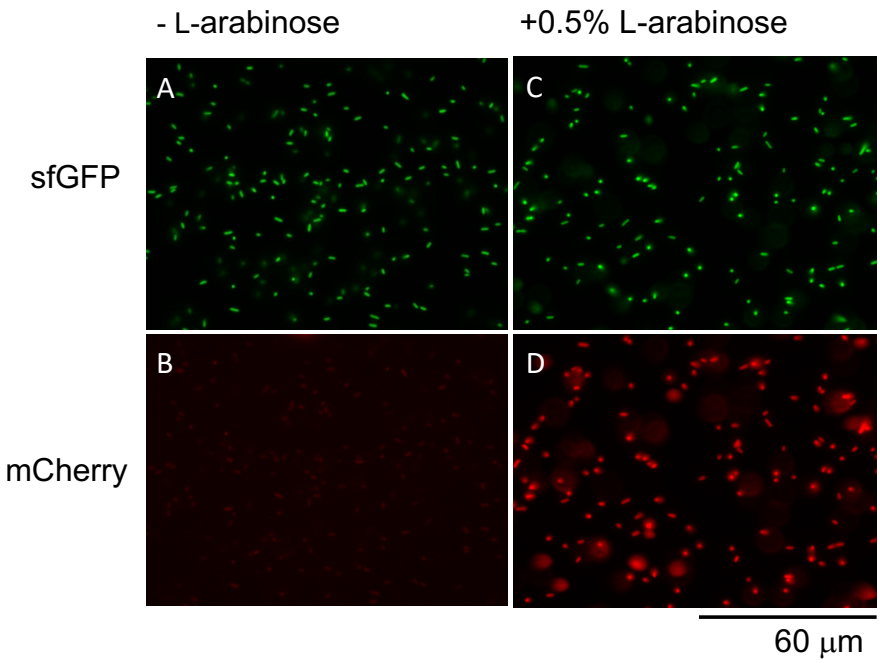


Figure 2.3: Fluorescence microscopy showing the induction of mCherry in liquid culture (LB medium) in the presence of 0.5% w/v L-arabinose after overnight growth. sfGFP is constitutively expressed in both conditions (A, C). mCherry is expressed in the presence of L-arabinose (D), minimal background fluorescence is observed in the in the absence of L-arabinose (B).

2.2.2 Growth of the E. coli strain in defined and rich medium

Here, we examined the advantages and disadvantages of defined minimal and undefined rich medium to determine optimal conditions for subsequent experiments.

There are two main advantages of defined minimal medium such as M9:

1) Minimal medium allows the tight control of each component which can be critical in determining conditions favourable for droplet stability. Droplet stability is one of the key challenges in the DIB field. In the next chapter we will investigate droplet stability in detail.
2) The comparatively low autofluorescence of M9 medium compared to LB medium (rich undefined medium) improves imaging of our sample. This allows us to see gene induction patterns more precisely.

However, rich medium provides more optimal conditions for cell growth. In the following experiments we examined the growth of our *E. coli* strain in both types of media to determine if rich medium (with the two main disadvantages shown above) is essential for consistent cell growth.

One challenge when using defined medium is the correct choice of carbon source. We examined the effect of addition of the commonly used carbon sources 0-0.4% w/v D-glucose and 0.4% w/v glycerol on the growth rate in liquid culture. We aimed to keep the D-glucose concentration as low as possible because it acts as a catabolite repressor, downregulating the L-arabinose operon (Ammar et. al, 2018). This also influences mCherry expression as it hinders full induction of the P_{BAD} promoter. If the level of D-glucose is kept too low, however, cell growth is hindered due to the lack of a suitable carbon source.

Expression of genomically integrated sfGFP was used as an indicator for cell growth. After 12 hours of growth a slight increase in growth rate was found at 0.4% w/v D-glucose concentrations with a mean fluorescence intensity of 4777 (± 534 a.u.) (Fig. 2.4). As shown in follow-up experiments the effect of catabolite repression was minimal at this D-glucose concentration (Fig. 2.6). We therefore chose 0.4% w/v D-glucose as a C-source in subsequent experiments as growth was maximised at this condition while minimising catabolite repression.

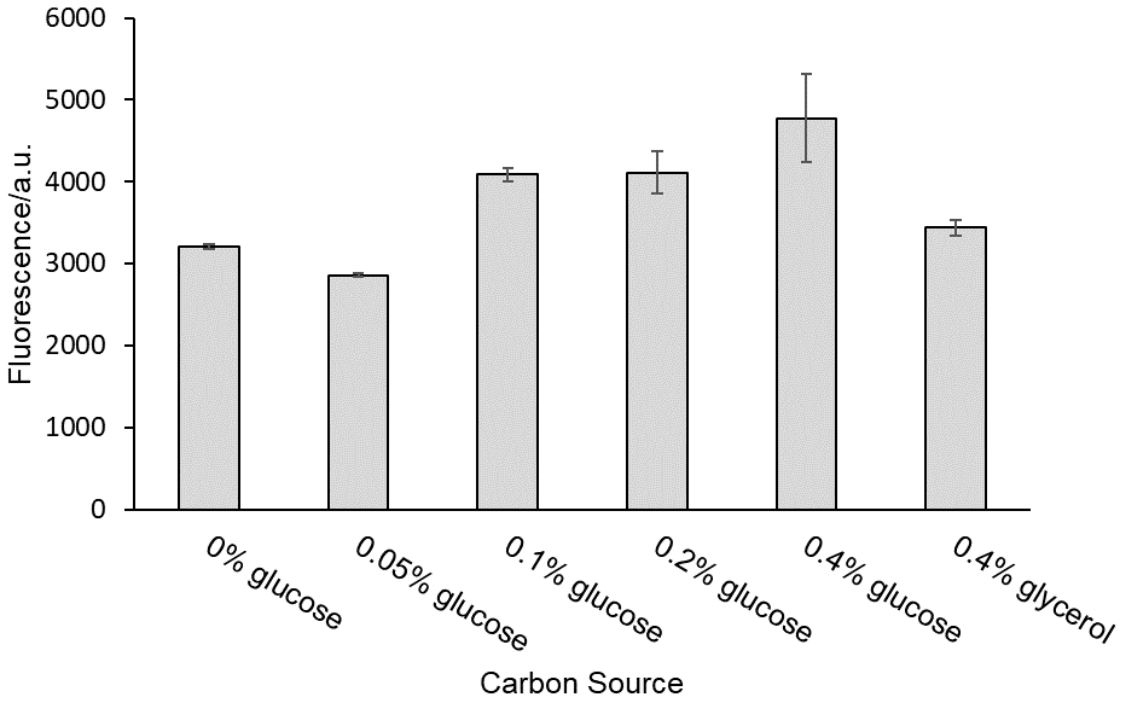


Figure 2.4: A bar chart depicting cell growth in M9 medium supplemented with 0-0.4% w/v D-glucose and 0.4% w/v glycerol. sfGFP expression was measured after a 12-hour period in liquid culture. Each point is the mean of 3 technical replicates. Error bars represent the standard deviation.

Next, we compared the growth rate and constitutive sfGFP expression of the *E. coli* strain in LB and M9 media. As expected, the growth rate was higher when cells were grown in LB medium, with the stationary phase of growth being reached after 4 hours compared to 11 hours for M9 medium. Similar, indirect conclusions about growth can

be drawn from the fluorescence data measuring constitutively expressed sfGFP, stationary phase is reached after 4h in LB and after 6h in M9 (Fig. 2.5).

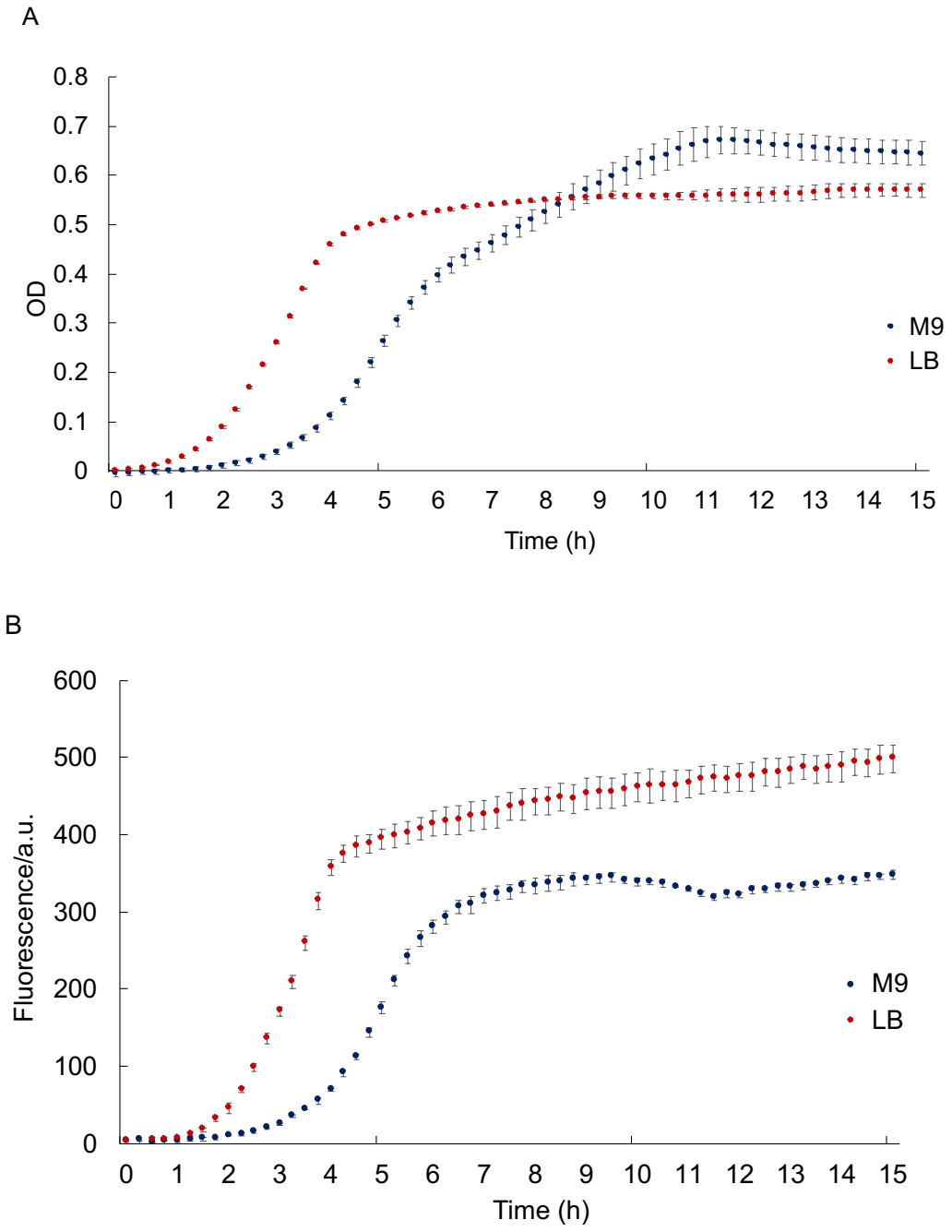


Figure 2.5: Plate reader data showing growth in rich and minimal medium. OD_{660} (A) and sfGFP expression (B) were measured in liquid culture over a 15-hour period in M9 and LB media. Cells constitutively express sfGPF. M9 media is supplemented with 0.4% w/v D-glucose. Healthy growth is observed in both conditions with a higher growth rate in LB. Each point is the mean of 3 technical replicates. Error bars represent the standard deviation.

From these experiments we concluded that, even though growth was slower in M9 medium compared to LB medium, the advantage of being able to control the exact contents of M9 medium outweighed this drawback. Additionally, as shown later, growth phases were sufficient for mCherry induction (see chapter 4).

2.2.3 mCherry induction in defined and rich medium

In addition to growth, we compared the induction of mCherry by the inducer L-arabinose during growth in LB and M9 medium. We grew the strain in liquid culture with and without the addition of 0.5% w/v L-arabinose and quantified mCherry induction after 8 hours of growth. In both types of medium, we observed negligible expression of mCherry in the absence of L-arabinose (Fig. 2.6). This indicates that the P_{BAD} expression system has a tight off-state. This is important in order to achieve patterned gene expression with droplet networks, the final goal of this project, as a clear difference between induced cells in proximity to the droplet network and non-induced cells exhibiting background fluorescence must be distinguishable. In the presence of L-arabinose we observed mCherry expression at high levels (Fig. 2.6). The observed fluorescence is higher when cells are grown in LB as compared to M9 medium with a mean fluorescence intensity of 1643 (± 583 a.u.) compared to 786 (±168 a.u.) fluorescent units, respectively. However, the level of mCherry induction in M9 was sufficient, to show a clear on/off state.

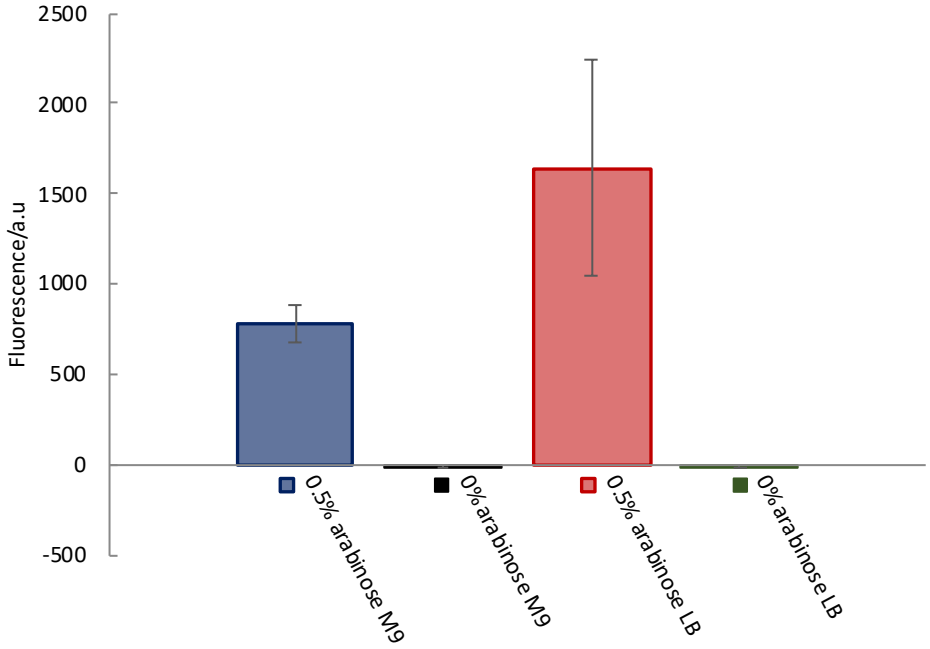


Figure 2.6: A bar chart showing the induction of mCherry in the presence and absence of 0.5% w/v L-arabinose. Cells were grown in liquid culture over a period of 12 hours. Each point is the mean of 3 technical replicates. Error bars represent the standard deviation. A t-test was carried out to compare the mCherry expression at 0.5% w/v L-arabinose to the control group (p= 0.0112, t = 4.4574, df = 4).

2.2.4 mCherry induction at varying L-arabinose concentrations

Next, we examined the induction of mCherry at a variety of inducer concentrations. An understanding of the conditions leading to mCherry expression is critical to anticipate the requirements that droplet networks must meet to locally induce gene expression in a gel containing bacterial cells. We observed significant induction after 4 hours, reaching its maximum level after 6 hours (Fig. 2.7). Importantly, mCherry expression increased with increasing inducer concentration up to a value of 0.5% w/v L-arabinose. A further increase to 1% w/v L-arabinose did not further increase mCherry expression. From this data we concluded that cells require exposure to a concentration of 0.5% w/v L-arabinose for optimal results. Importantly, we carried out these experiments in liquid culture whereas subsequent gene induction experiments

with droplet networks were carried out in an agarose gel. This could influence both the rate of mCherry expression as well as the concentration of inducer needed to reach maximum induction. However, these results served as an initial indication of optimal conditions for further experiments in Chapters 3 & 4.

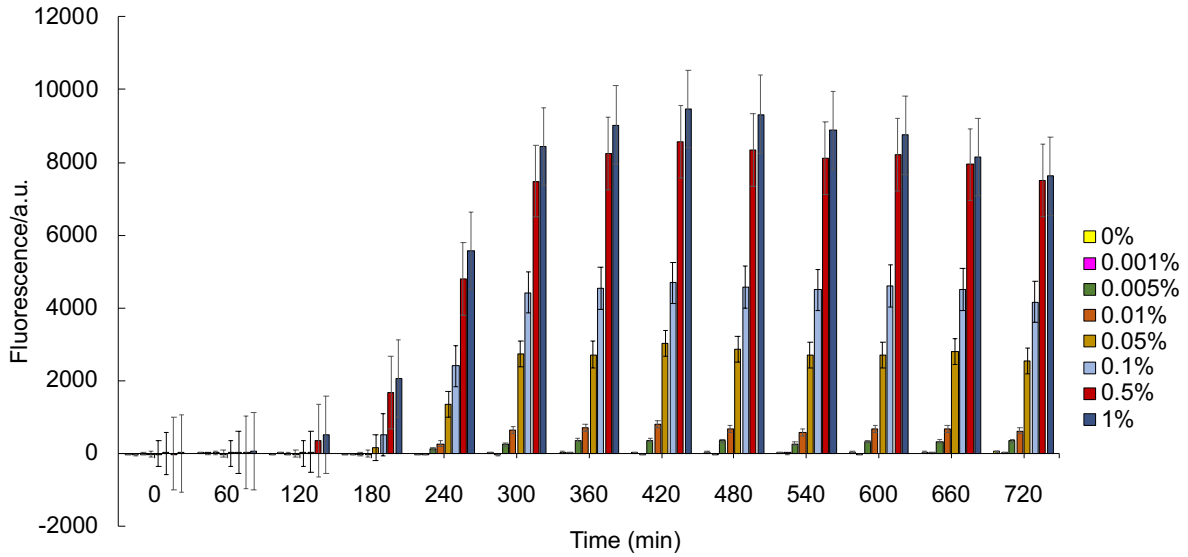


Figure 2.7: Plate reader data showing the induction of mCherry at varying concentrations of L-arabinose (in w/v). M9 growth medium was supplemented with the inducer at the beginning of the experiment. Cells were grown in liquid culture over a period of 9 hours. Each point is the mean of 3 technical replicates. Error bars represent the standard deviation. A t-test was carried out to confirm that further increasing the L-arabinose concentration from 0.5% w/v to 1% w/v did not significantly increase mCherry expression after 720 minutes ($p= 0.1942$, $t = 1.558$, $df = 4$).

2.2.5 Forming a uniform agarose gel containing embedded *E. coli* cells

The formation of a uniform gel layer with embedded bacteria in an experimental setup that can be filled with a lipid/oil solution is an essential requirement to proceed to later stages in the project. A lipid-oil-environment is required to form stable droplet networks with a bilayer at the droplet-hydrogel interface.

Over the course of the project, we explored several experimental setups (Fig. 2.8). Setup 1 consists of an agarose-covered glass slide with a plastic ring placed on top (Fig. 2.8 A, B). We performed agarose-coating by pipetting a molten agarose solution on a clean glass slide before adding the plastic ring on top of the slide. The ring formed a chamber for the addition of the lipid/oil solution. A lipid monolayer then formed between the hydrogel and the lipid/oil phase.

However, this method suffers from several downsides. Firstly, we placed the plastic ring on the hydrogel before gelation. Theoretically, this leads to the ring being embedded in the gel and forming a seal that prevents the lipid/oil solution from leaking onto the hydrogel. In practice, the resulting seal was imperfect, and we observed leakage of the oil solution in around 70% of cases. Secondly, formation of the hydrogel and addition of the plastic ring required around 30 minutes of assembly time, which was too low throughput for running experiments.

Setup 2 consists of a quartz cuvette that was covered with the hydrogel layer at the bottom of the well (Fig. 2.8 C). We simply pipetted warm pre-gel (67°C) into the chamber before placing the cuvette in the fridge for gelation (5°C). We then added the lipid/oil solution to the cuvette. To enable a higher throughput of our experiments, we used 8-well Nunc Slides allowing us to perform up to 8 experiments on one slide (Thermo Fisher) (Fig. 2.8 D). The time it took to form the hydrogel was also drastically reduced to around 2 minutes. The quartz cuvette and Nunc Slides used in

setup 2 consisted of quartz and glass bottoms respectively. Importantly, this untreated hydrophobic surface did not allow for the formation of a uniform gel layer (Fig. 2.8 F). Therefore, we plasma cleaned the chambers before the addition of the hydrogel to generate a hydrophilic surface (by hydroxylating the glass surface) that allowed the hydrogel to evenly spread throughout the bottom of the well (Fig. 2.8 E).

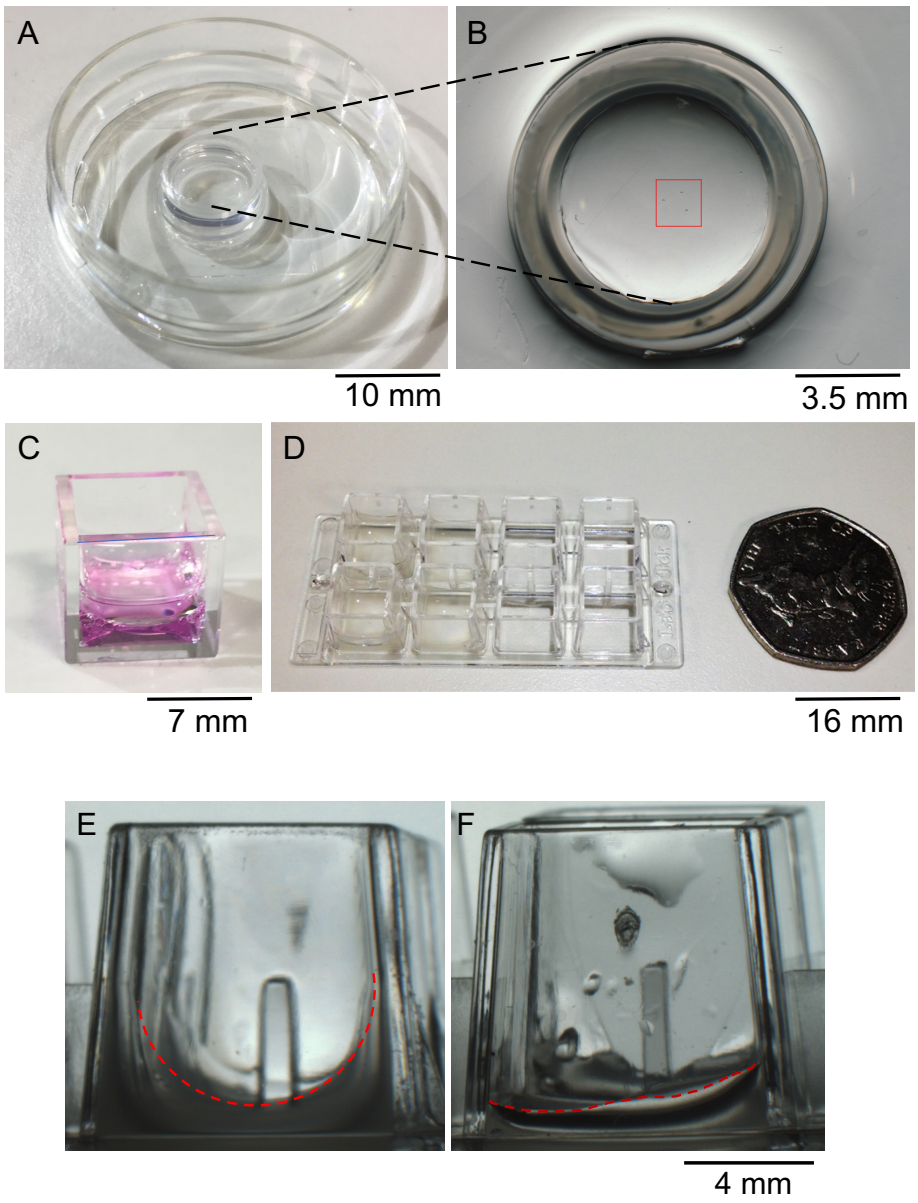


Figure 2.8: Images of the experimental setups tested in this project. Experimental setup 1 consisted of a hydrogel-covered glass slide. The glass slide was placed inside a Petri dish (A). A plastic ring was then placed in top of the gel layer and filled with a lipid/oil solution. Three aqueous droplets with a diameter of 180 μm were

placed inside the chamber and are highlighted in red (B). Experimental setup 2 consisted of a quartz cuvette. (C). 8-well Nunc slides allowed for the parallelisation of experiments (D). Plasma cleaning was required to achieve an even hydrogel layer. Addition of hydrogel without plasma cleaning resulted in uneven gel formation (F). Addition of the hydrogel after plasma cleaning resulted in evenly spread hydrogels (E). The edge of the hydrogel is highlighted in red.

2.2.6 Optimising the gel thickness for imaging quality

In addition to ensuring that the hydrogel covers the bottom of the chamber evenly, we optimised the thickness of the gel for imaging. Ideally, the cells cover the well completely without being too dense, to obtain a clear image on the fluorescence microscope. To achieve this, we aliquoted different volumes of hydrogel containing *E. coli* cells into the wells after plasma cleaning. The volumes we added ranged from 20-160 μL. We then imaged the well after overnight growth. Cells grew into individual colonies that could be observed using fluorescence microscopy. At volumes under 100 μL the bottom of the well was not covered entirely with the cell layer (Fig. 2.9 A, B). At volumes over 120 μL, the thickness of the gel resulted in unclear images due to increased background fluorescence from cells underneath the plane of focus (Fig. 2.9 E, F). At a volume of 120 μL, colonies of cells were clearly distinguishable without excessive background fluorescence while at the same time completely covering the bottom of the well (Fig. 2.9 C, D). We measured the thickness of the 120 μL hydrogel layer to be 150-200 μm using confocal microscopy. We continued to use this volume of hydrogel in all subsequent experiments.

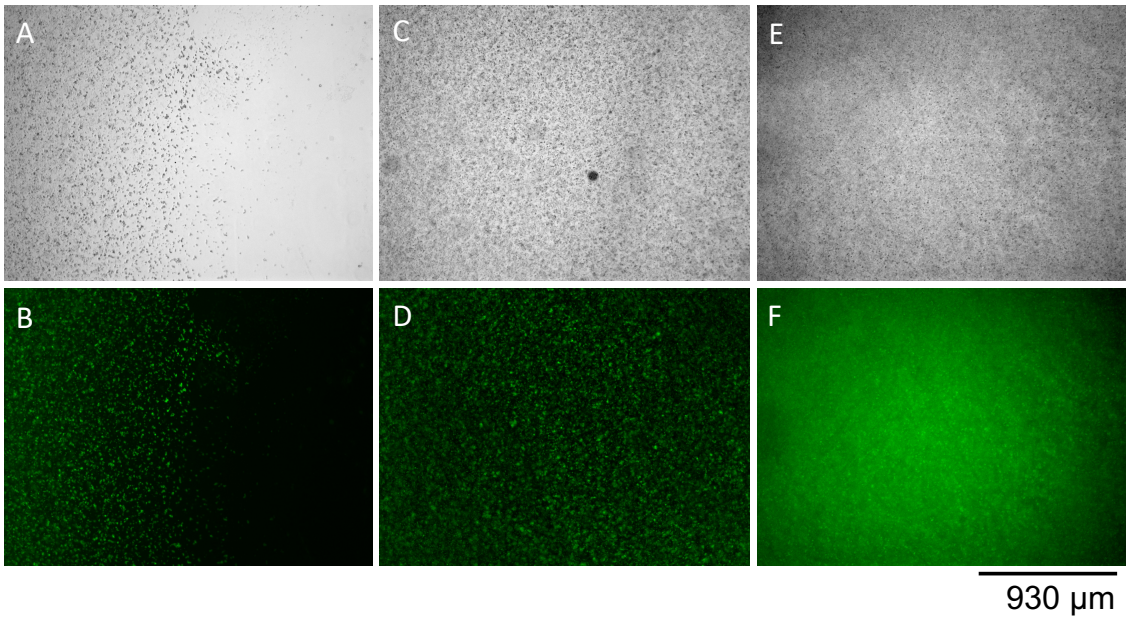


Figure 2.9: Bright field and fluorescence microscopy images showing the distribution of cells at varying gel thicknesses. Different volumes of cell-containing hydrogel were added to the experimental well and imaged after overnight growth. At volumes of under 100 μL cells do not cover the bottom of the well completely exposing the glass bottom (A), (B). At 120 μL volume a thin hydrogel layer completely covered the well (C), (D). At volumes of over 120 μL, substantial background fluorescence from 3D stacking of cells was observed (E), (F).

2.2.7 The effect of a lipid-oil-solution on cell growth in a submerged hydrogel

We investigated whether the addition of the oil solution to the *E. coli* embedded hydrogel altered the growth conditions of the *E. coli* cells such as by limiting oxygen diffusion to the cells. To determine these effects, we compared cell growth in wells with and without the addition of 150 µL of oil (35:65 v/v ratio of undecane-to-silicone oil). We then measured constitutive sfGFP expression as an indication for cells growth after 18 hours of incubation at 37°C. Although cell-containing hydrogels that were submerged in oil did show higher variability in growth between replicates, we did not find a significant difference between wells that did and did not have a layer of

oil phase covering the hydrogel (Fig. 2.10), confirming a negligible effect of the oil phase on the growth of *E. coli* cells.

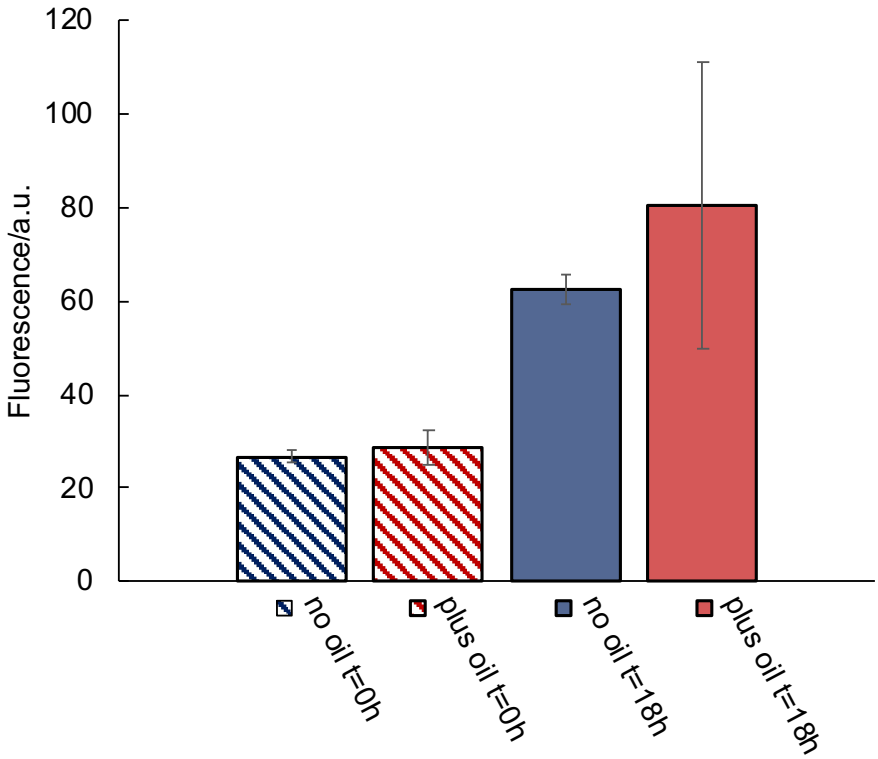


Figure 2.10: A bar chart showing cell growth in an agarose-based hydrogel with and without the addition of an oil phase covering the gel. Cells were grown at 37°C over a period of 18 hours. Each point is the mean of 3 technical replicates. Error bars represent the standard deviation. A t-test was carried out to confirm that there was no significant difference in sfGFP expression between the experimental and the control ($p= 0.5024$, $t = 0.7362$, $df = 4$)

2.2.8 Preventing dehydration of the hydrogel layer

Induction of gene expression using synthetic tissues requires coincubation of bacterial cells and droplet networks at 37°C for several hours. Over this period of time the 150 μm thick gel is subject to dehydration by evaporation of water through the oil phase. Dehydration leads to shrinking of the hydrogel layer, causing it to

buckle and rip. This prevents the droplet network from steadily exposing cells to a local concentration of inducer. One potential solution to this problem is to reduce the incubation temperature from 37°C to 25°C. This drastically reduced dehydration of the hydrogel. However, as expected, cell growth was also significantly reduced (Fig. 2.11). Bacterial colonies appeared smaller in hydrogels incubated at room temperature compared to incubation at 37°C. Another solution to the problem is to provide the experimental chamber with high humidity during the incubation period. We achieved this by enclosing the well in a water filled container. Hydrogels incubated at 37°C at high humidity exhibited strong cell growth while preventing dehydration over the 18-hour period. We used these conditions in further experiments.

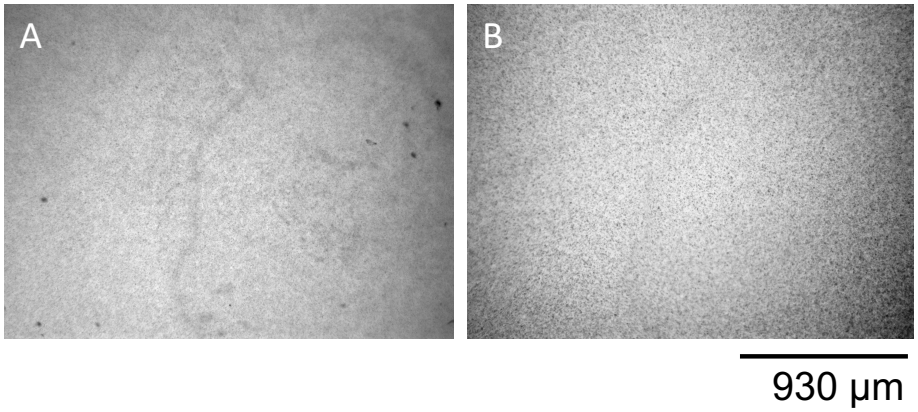


Figure 2.11: Cell growth in an agarose-based hydrogel after 18 hours of incubation. Hydrogels grown at room temperature exhibited a significant reduction in growth which results in small colony sizes (A). Hydrogels grown at 37°C were enclosed in a water filled chamber that provided a high humidity environment. The resulting hydrogel were densely covered with large colonies (B). Both hydrogels were seeded with the same number of cells. Images shown here are representative of 3 technical replicates.

2.2.9 mCherry induction under coincubation conditions

In the final experiment in this chapter, we tested mCherry induction under the following conditions: a 150-200 μm thick bacteria-containing hydrogel layer, 18-hour incubation at 37°C and covering the hydrogel with a lipid/oil solution. These are the conditions required for experiments including droplet networks (see chapter 4). To test if our bacterial strain expresses mCherry under these conditions, we mixed 0.5% w/v L-arabinose into the hydrogel at t = 0 (Fig. 2.12).

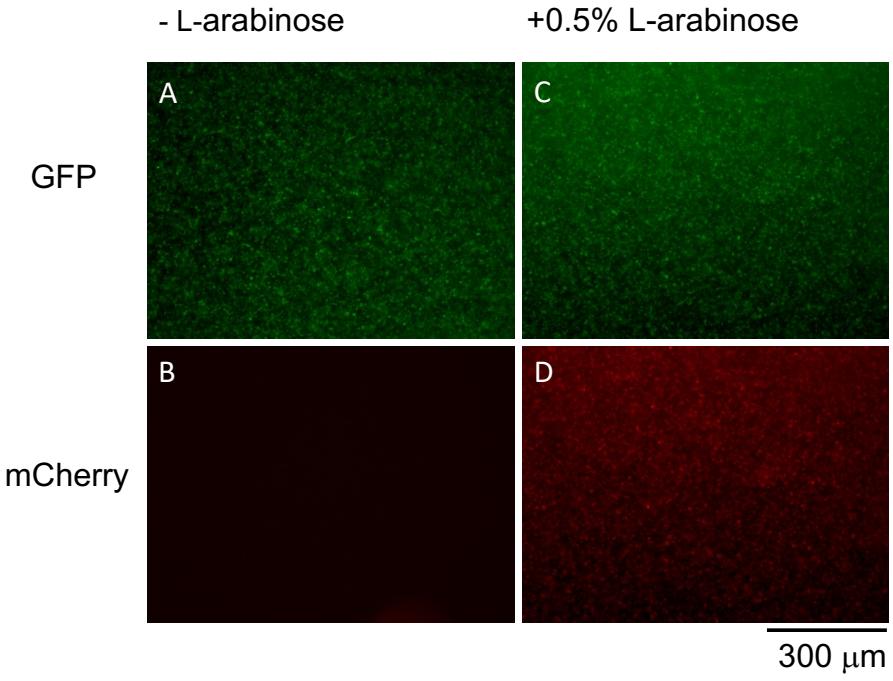


Figure 2.12: Fluorescence microscopy images showing mCherry induction in a 150-200 μm thick gel, covered in an oil solution after 18 hours of incubation at 37°C. Cells are uniformly distributed (A), (C). mCherry is expressed in the presence of 0.5% w/v L-arabinose (D). Negligible background fluorescence is observed in the absence of the inducer (B).

Finally, we quantified mCherry expression from the fluorescence microscopy images in Fig. 2.12. To do this we measured and compared mCherry expression at t = 0 and after 18 hours of incubation at 37°C. We observed a high level of induction in the presence of 0.5% w/v L-arabinose with a mean fluorescence intensity of 362 (± 534 a.u.) compared to a mean fluorescence intensity below 50 a.u. in all other conditions (Fig. 2.13).

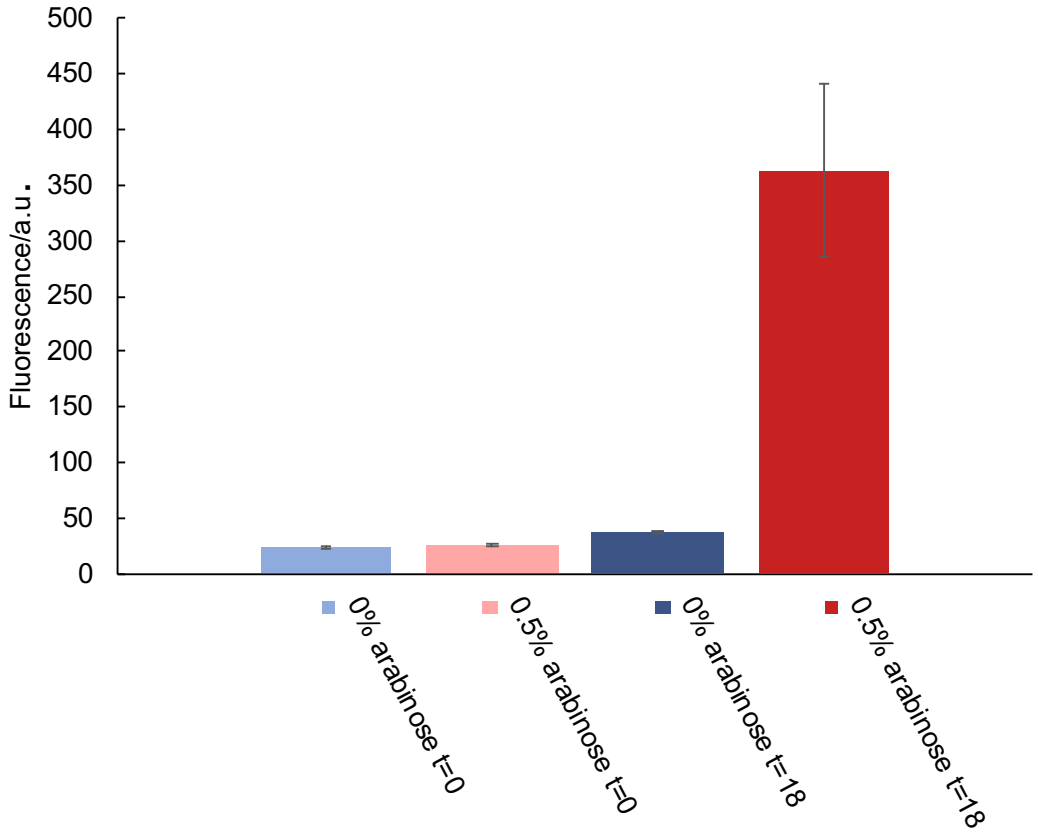


Figure 2.13: A bar chart quantifying mCherry induction in a 150-200 μm thick gel, covered in an oil solution, at t = 0 and after 18 hours of incubation at 37°C. Cells were exposed to 0 or 0.5% w/v L-arabinose. At t = 0 no mCherry expression was observed. After 18 hours mCherry was expressed in the presence of L-arabinose. Each point is the mean of 3 technical replicates. Error bars represent the standard deviation. A t-test was carried out compare mCherry induction in the presence of 0.5% L-arabinose and the control group (p= 0.0007, t = 9.6236, df = 4).

2.3 Summary

In this chapter we investigated the biology and experimental setup behind the end goal of this project. We showed that the bacterial strain grew robustly in M9 minimal medium supplemented with 0.4% w/v D-glucose and within an agarose hydrogel layer formed with the same nutrients. The bacterial cells containing mCherry under the control of the P_{BAD} expression system expressed the fluorescent protein optimally at L-arabinose concentrations of above 0.5% w/v. We established an experimental setup that allows for the coincubation of the bacterial strain and droplet-based systems. Importantly we showed that mCherry is expressed when cells are grown in a hydrogel submerged in an oil solution in this experimental setup.

2.4 Materials & Methods

2.4.1 Bacterial strains

The *E. coli* strain BZB1011 *sfgfp*::*Tn7* in this project was previously used in work from our group (Krishna Kumar et al., 2020). It contained constitutively expressed sfGFP that was genomically integrated at the Tn7 site.

2.4.2 Preparation of bacterial media

Lysogeny broth Miller (LB) medium (Sigma-Aldrich) was prepared using standard protocols (Sambrook et al., 1989). 5x M9 salts (Sigma-Aldrich) were prepared using standard protocols: 8.46 grams were diluted in 150 mL of Milli-Q® water. The solution was supplemented with 2 mM $MgSO_4$ and 0.1 mM $CaCl_2$ that were previously filter sterilized using a 0.22 µm cellulose acetate membrane filter (Corning). Additionally, the medium was supplemented with 0.2% w/v casamino acids (Sigma) and varying concentration of D-glucose (0.05, 0.1, 0.2 & 0.4 % w/v) and 0.4 % w/v of glycerol, to create our minimal M9 medium. The solutions were autoclaved and stored at room temperature for up to 4 weeks. The growth medium was supplemented with 100 µg mL^{-1} of ampicillin.

OD_{600} and fluorescence measurements were carried out in a plate-reader (CLARIOStar, BMG Labtech, Germany). During growth, each well in 96-well plates (Corning, product number 3595) were filled with 200 µL of media and incubated at 37°C with shaking at 400 rpm. Wells were inoculated with a starting OD_{660} of 0.01 from overnight cultures.

During L-arabinose screening, the inducer was dissolved in M9 medium, and filter sterilised before inoculation.

2.4.3 L-arabinose responsive Plasmid

The genetic construct used in this work was previously constructed in the Bayley group. The red fluorescent protein mCherry is placed under the control of the L-arabinose responsive P_{BAD} promoter. The plasmid contains the transcription factor AraC and an ampicillin resistance cassette. The *E. coli* strain BZB1011 *sfgfp*::*Tn7* was prepared to be chemically competent using standard protocols (Krishna Kumar et al., 2020). Briefly, after overnight growth in LB medium, cells were inoculated at an OD_{600} of 0.05 and grown at 37°C to an OD_{660} of 0.4. 25 mL of cultures were centrifuged at 4°C at 1734g for 10 minutes. Supernatant was discarded and pellets were resuspended in 12.5 mL of 100 mM $CaCl_2$ & 15% v/v glycerol. Cells were cooled on ice for 45 minutes and centrifuged again. After resuspension in 5 mL of 100 mM $CaCl_2$ & 15% v/v glycerol, cells were frozen and stored at -80°C.

The L-arabinose responsive plasmid was transformed with a heat shock protocol (Froger & Hall, 2007). 100 µL of competent cells were thawed on ice and 100 ng of plasmid was added to each tube. The mixture was then heat shocked by transferring them into a water bath at 42°C for 45 seconds. Cells were placed on ice for 2 minutes and recovered by adding 100 µL of LB medium. After 1 hour of incubation at 37°C, 100 µL of the solution was plated onto selective LB-plates (1.5% w/v).

2.4.4 Preparation of the lipid/oil solution

25 mg of powder of the lipids 1,2-diphytanoyl-sn-glycero-3-phosphocholine (4ME 16:0 PC (DPhPC)) and 1-palmitoyl-2-oleoyl-sn-glycero-3-phosphocholine (16:0-18:1 PC (POPC)) was purchased from Avanti Polar Lipids and dissolved in chloroform. The two solutions were mixed resulting in a 2:1 DPhPC:POPC molar ratio. The solution was aliquoted into previously cleaned glass vials (Supleco®), dried under a nitrogen stream to produce a lipid film by evaporation of chloroform. Films were then

desiccated under vacuum for 18 hours, sealed using polytetrafluoroethylene (PTFE) film tape and stored at -80°C under argon gas.

Before use, the lipid film was kept at room temperature for 30 minutes. A filtered (0.22 µm cellulose acetate membrane filter (Corning)) oil solution containing undecane (Sigma-Aldrich) and Silicone Oil AR20 at a 35:65 ration by volume was added to the film resulting in a 2 mM lipid concentration. The resulting lipid/oil solution was sonicated for 1 hour before use.

2.4.5 Preparation of the bacteria-containing hydrogel layer

After inoculation from glycerol stocks, cells were grown overnight in LB medium. This solution was used to inoculate 4 mL of LB medium until an OD_{600} of 1.2 was reached. 916 µL of this culture was then centrifuged for 8 minutes at 8000 g. The excess supernatant was discarded, and the pellet was resuspended in a hydrogel solution containing autoclaved M9 medium and 1.5% w/v ultra-low gelling temperature agarose at 67°C (Sigma-Aldrich). The final solution contained ≈ 10^9 cells mL^{-1}.
120 µL of the pregel solution was then aliquoted into 8-well Nunc slides (Thermofisher) that were treated in an O_2 plasma cleaner for 5 minutes. After addition of the hydrogel slides were cooled to 5°C for 15 minutes. After addition of 150 µL of lipid/oil solution, Nunc slides were placed inside a plastic container filled with Milli-Q® water to ensure sufficient hydration and kept inside an incubator at 37°C overnight.

2.4.6 Image analysis

Imaging was performed on a Leica DMi 8 epi-fluorescence microscope at 5x or 40x magnification. The exposure and gain were kept constant between experiments. Image analysis was performed using Fiji (ImageJ).

3 Gene induction using single droplets

3.1 Introduction

In the previous chapter, we characterised the L-arabinose-responsive expression system. Additionally, we developed an experimental setup that allows for the co-incubation of a bacterial-containing hydrogel and a droplet network. In this chapter, we explore the stability of systems based on single aqueous droplets and their ability to induce gene expression. Single droplets serve as a simplified model system for 3D-printed droplet networks consisting of hundreds of interconnected droplets, allowing us to quickly characterise our experimental setup. In this chapter we investigate the transfer of a fluorescent dye between droplets to better understand experimental parameters that influence the insertion of the αHL pore. We characterise the droplet hydrogel bilayer (DHB) experimental setup by investigating the formation and size of bilayers between the droplets and the hydrogel. We examine the stability of a single droplet on top of the bacterial-containing hydrogel layer and the controlled release of initiators as well as fluorescent counterparts from the droplet to the hydrogel layer. These experiments serve as model for subsequent release of an inducer from single droplets and droplet networks.

3.2 Results and Discussion

3.2.1 Controlling bilayer permeability with αHL

For our system we need to be able to control the release of the inducer (L-arabinose) from the droplet networks into the hydrogel layer (containing embedded bacteria) to achieve localised gene induction patterns. One way to achieve this goal is to permeabilise the lipid bilayers to control the transport of the inducer through the bilayers. We chose the protein pore αHL for bilayer permeabilisation and investigated the transfer of a fluorescent L-arabinose analogue through a DIB formed between a pair of droplets and permeabilised by αHL (Fig. 3.1, 3.2). For our fluorescent L-arabinose analogue, we used 7-nitrobenzofurazon(NBD)-glucose because of its structural similarities. In the droplet pair, the left droplet contained 1 mM NBD-glucose and 10 mM Tris-HCl buffer and the right droplet contained 10 mM Tris-HCl buffer and 0.1 mg αHL (Fig. 3.1, 3.2). After 18 hours, the NBD-glucose – that was originally compartmentalised in the left droplet – had equilibrated across both droplets. When droplet pairs did not contain αHL, NBD-glucose remained compartmentalised the left droplet after 18 hours (Fig. 3.1, 3.2). Our combined results confirmed permeabilization of the bilayer by αHL insertion, which facilitates the transport of NBD-glucose through the protein pore, as well as demonstrating controlled release of an inducer analogue through a bilayer.

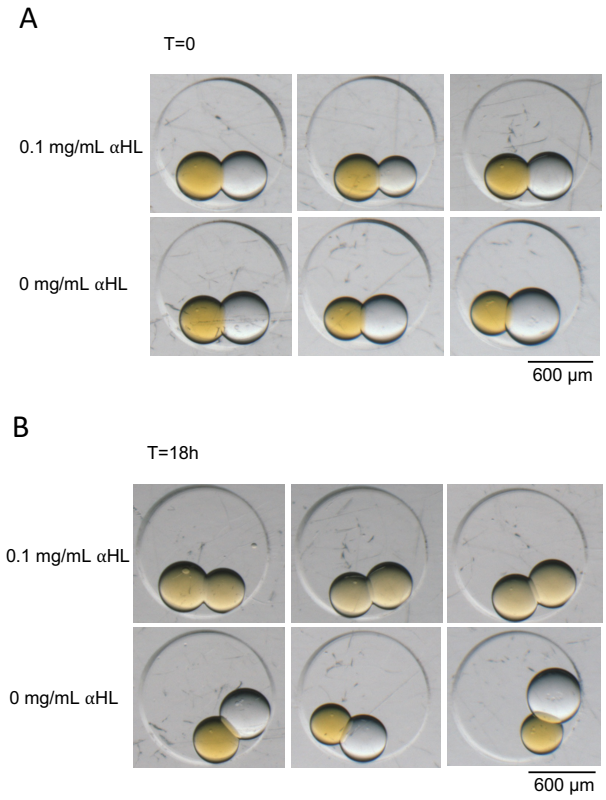


Figure 3.1: Light microscope images showing the transfer of the fluorescent dye NBD-glucose between a DIB in the presence of the protein pore αHL. DIBs were formed between droplets containing buffer & αHL and droplets containing 1mM NBD-glucose and buffer. The control group did not contain αHL. Images are taken at the beginning of the experiment (A) and after an 18-hour period (B).

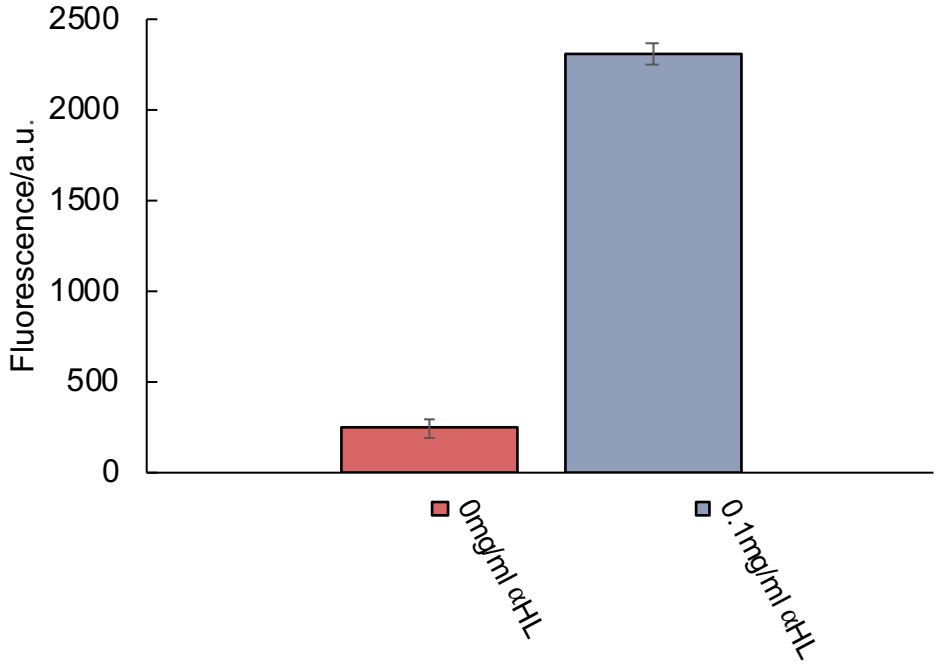


Figure 3.2: A bar chart quantifying dye transfer between a DIB in the presence of the protein pore αHL. An increase in mean fluorescence after an 18-hour incubation period indicated the diffusion of NBD-glucose across the DIB in droplet pairs that contained αHL (shown in blue). Droplets pairs that did not contain αHL showed no increase in mean fluorescence (shown in red). Each point is the mean of 4 technical replicates. Error bars represent the standard deviation. A t-test showed a statistically significant difference between the experimental and control group (p= 0.0001, t = 57.9313, df = 6).

3.2.2 Optimising αHL insertion

From our experiments in 3.2.1, we qualitatively noticed that the incubation time of a droplet – the time an aqueous droplet is in the lipid/oil solution before it is brought in contact with another droplet to form a DIB – affected the rate of dye transfer in droplets that contained αHL. In previous work, longer incubation times (15 – 30 mins) increased the stability of a DIB (Leptihn et. al, 2013). However, we hypothesised that this incubation time, had an effect on the insertion of the αHL into bilayers and subsequent pore formation. To investigate this, we performed experiments where we compared the incubation times of 0 minutes and 30 minutes between droplets pairs

containing αHL and measured dye transfer (Fig. 3.3.). Interestingly droplet pairs without an incubation period had much faster dye transfer rates (complete dye transfer after 4 hours) than droplet pairs with a 30 minute incubation time (40% of dye transfer after 4 hours and complete dye transfer after 18 hours) (Fig. 3.4). Our results show that longer incubation times reduce the rate of dye transfer – mediated by transport through αHL pores – between droplets. We assume reduced rates of dye transfer is because of fewer αHL pores in the bilayer after longer incubation periods. Mechanistically, we hypothesise that longer incubation time allows for greater aggregation of the αHL monomer at the water-oil interface, resulting in potential disruption of the monomer secondary structure, which would result in a lower effective αHL concentration once bilayers are formed. Previous work suggests an alternative hypothesis: prolonged incubation times lead to the formation of stacked lipid structure at the water-oil interface preventing proper DIB formation (Leptihn et. al, 2013). Investigation of the mechanism behind reduced αHL pores with longer incubation times was beyond the scope of this work and requires further study.

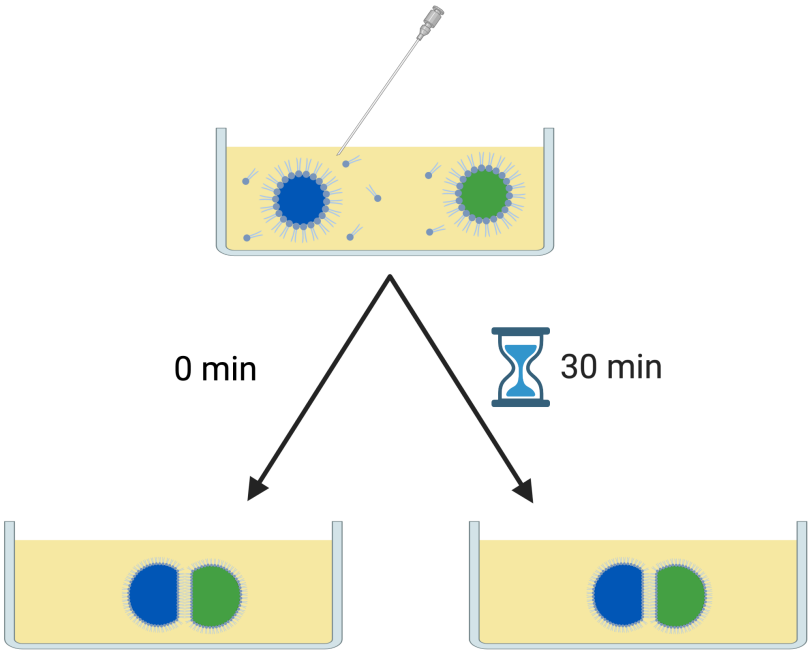


Figure 3.3: Diagram depicting the experimental procedure to investigate the effect of incubation time on dye transfer across a DIB. After droplet formation in the lipid/oil solution, DIBs are formed immediately or after a 30-minute incubation period.

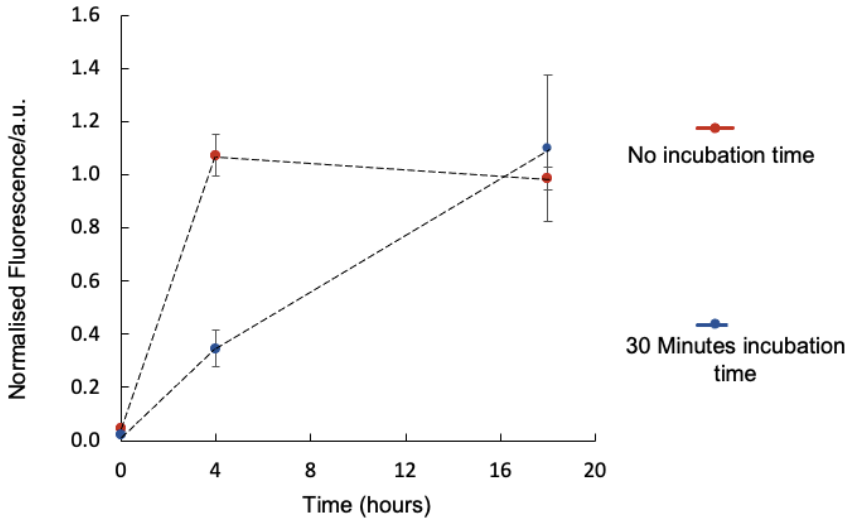


Figure 3.4: A scatter plot depicting the effect of incubation time on dye transfer across a DIB. Mean fluorescence in buffer droplets normalised to the mean fluorescence in the corresponding dye-containing droplet in droplet pairs. Red data points show mean fluorescence in droplet pairs without incubation before DIB formation. Blue data points show the mean fluorescence in droplet pairs with a 30-minute incubation period before DIB formation. Each point is the mean of 3 technical replicates. Error bars represent the standard deviation.

3.2.3 Investigating droplet stability and contact angles in DHBs

After showing that NBD-glucose could be transferred between a droplet pair, we investigated the formation and stability of DHBs.

Droplets (180 µm in diameter) were added to a lipid/oil solution on top of a hydrogel (see Chapter 2 for formation of the agarose hydrogel). After addition, droplets sink to the bottom of the lipid/oil solution leading to the formation of a bilayer between the droplet and the hydrogel.

As shown in previous work, composition of the oil phase has an impact on the contact angle between droplets, a reflection of the DIB size (Alcinesio et al., 2020). The study showed that increasing the volume fraction of silicone oil (φ_{SIL}) in an undecane-silicone oil mixture increases the contact angle between droplets.

In the experiments shown here we investigated the same effect in droplet hydrogel bilayers. There are two main characteristics of our setup that are influenced by the contact angle. First, a larger contact angle increases the bilayer size and thus allows for increased insertion of αHL into the DHB. Second, variations in contact angle influence droplet stability.

Contact angles, the angle formed between the droplet and hydrogel, were calculated by measuring the radii of the DHB and the truncated droplet (see Fig. 3.5 for definition of variables) and using Equation 1 (Alcinesio et al., 2020):

$$Contact\ angle\ (°) = sin^{-1}\left(\frac{R_a}{R_b}\right)$$

As previously show with DIBs, we found that increasing φ_{SIL} increased the size of the DHB formed between the droplet and the hydrogel (Fig. 3.6). Larger bilayer sizes

would allow for the incorporation of more αHL pores, and subsequently, faster inducer transfer rates. However, we found the largest DHB formed (φ_{SIL} = 0.75, θ = (63° ± 5) (Fig. 3.6D), greatly decreased the stability of the droplet to a few hours compared to days for smaller DHB sizes (φ_{SIL} = 0.50, θ = (42° ± 3), φ_{SIL} = 0.25, θ = (25° ± 1)). For further experiments, we found a compromise by using a φ_{SIL} = 0.50, which provided sufficiently large DHBs, and a stable droplet over several days.

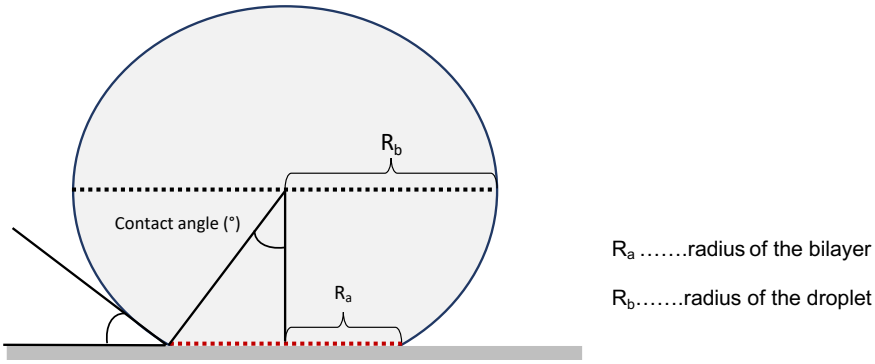


Figure 3.5: A diagram showing the terms used in Equation 1 to calculate the contact angle (°) between a droplet and a hydrogel in a DHB.

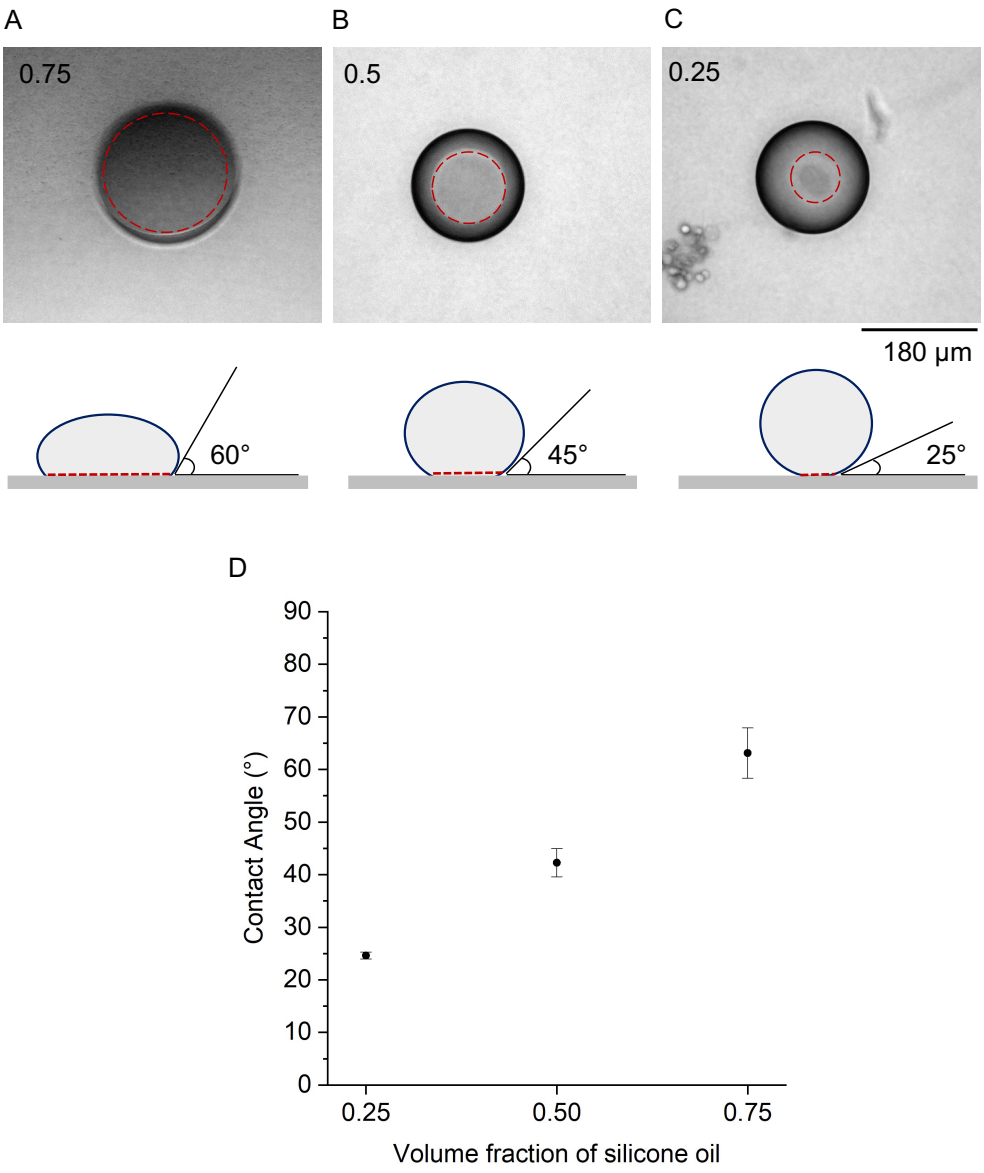


Figure 3.6: Composition of the lipid/oil phase results in variations in the contact angles between droplets and the hydrogel. The ratio between undecane and silicone oil was tested at φ_{SIL} = 0.75 (A), φ_{SIL} = 0.5 (B) and φ_{SIL} = 0.25 (C). Microscopy images in the top row depict bilayer sizes at equilibrium contact angles. Illustrations in the bottom row depict the relationship between contact angles, the shape of droplets and resulting bilayers. The edges of the bilayers are shown in red. The bottom figure shows the quantification of the effect of oil-phase composition on the equilibrium contact angle (°) in DHBs (D). The three tested conditions are described above. Each point is the mean of 4 technical replicates. Error bars represent the standard deviation.

3.2.4 Release of dyes into the hydrogel layer

Next, we investigated the diffusion of NBD-glucose from single droplets into a hydrogel layer through αHL-permeabilised DHBs. These experiments served as a model for diffusion of L-arabinose from droplets (Fig. 3.10) Firstly, we examined the effect of incubation times on NBD-glucose diffusion, by tracking the fluorescence intensity in droplets over a 1-hour period. Droplets (180 μm in diameter) contained buffer, 100 μM NBD-glucose, and 0.1 mg/mL αHL, and were incubated for 0 and 30 minutes respectively before DHB formation. With no incubation time, droplets that contained the protein pore rapidly decreased in fluorescence (after 15 mins the fluorescence intensity had dropped to 34% (± 17)), confirming that NBD-glucose diffuses across the DHB. After 45 minutes the dye was completely released from the aqueous droplet into the hydrogel. Importantly, when droplets did not contain αHL the fluorescence stayed constant over the 1-hour period, demonstrating that insertion of the protein pore into the bilayer is required for rapid dye release. With a droplet incubation time of 30 minutes, dye diffusion was much slower (after 45 minutes the fluorescence intensity was 74% (± 5), confirming the effect of incubation times on αHL inhibition, as seen in section 3.2.2. Overall, our experiments showed that NBD-glucose can be released from an aqueous droplet into a hydrogel, and suggested that we would observe similar rates of diffusion when releasing the inducer L-arabinose in gene induction experiments.

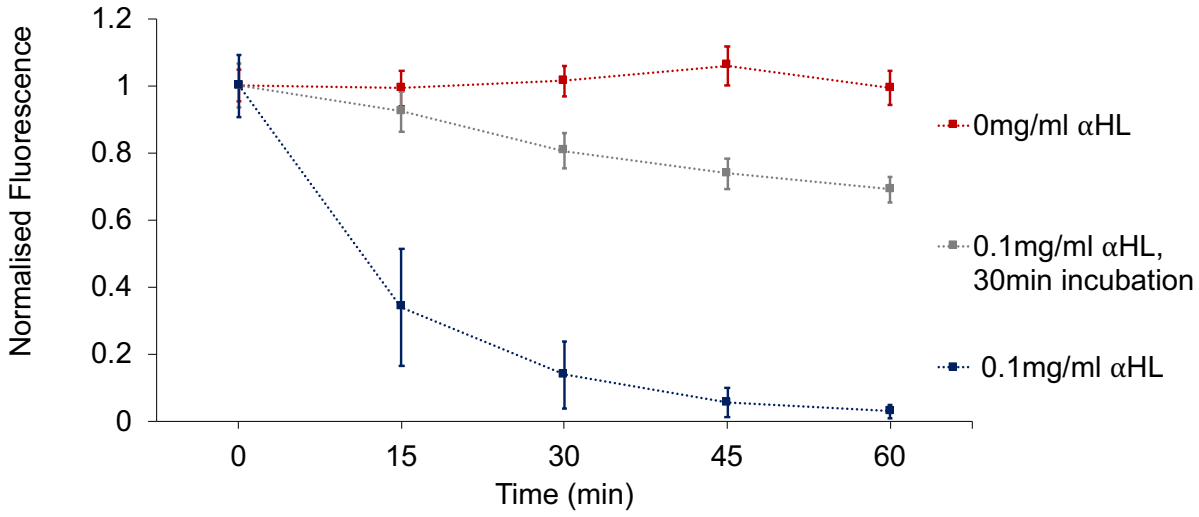


Figure 3.7: Release of NBD-glucose from aqueous droplets into a hydrogel layer. The mean fluorescence in each droplet was normalised to its initial fluorescence at t = 0. Aqueous droplets shown in blue contained 0.1 mg/mL of the protein pore αHL. The control group shown in red did not contain the protein pore. A third group contained the protein pore but was incubated in the lipid/oil solution for 30 minutes before the addition to the hydrogel is shown in grey. Each point is the mean of 4 technical replicates. Error bars represent the standard deviation.

Next, we investigated the rate of release of NBD-glucose from droplets into a hydrogel by controlling the concentration of αHL, and in turn, the number of pores in the DHB. We formed DHBs with droplets containing NBD-glucose and a range of αHL concentrations (1 – 100 μg/mL) and tracked the fluorescence intensity of the droplet over a 16-hour period. The results showed that the rate of release of the dye can indeed be controlled by altering the concentration of αHL (Fig. 3.8), such that decreasing concentrations of αHL results in decreased rates. At 0.1 μg/mL, a slight decrease in fluorescence to 96% is observed over the 16 hour period suggesting that NBD-glucose leaks into the hydrogel at a low rate. For 100 μg/mL αHL, the dye completely diffused out of the droplets. At concentrations at 1 and 10 μg/mL αHL, 94% (± 2) and 74% (± 5) of the fluorescence is retained after the 16-hour period.

From our results, the greatest control on the rate of release of small molecules appears to be from 10-100 μg/mL concentrations. Future work could further screen conditions in this range, potentially allowing us to accurately set the period of release of comparable molecules.

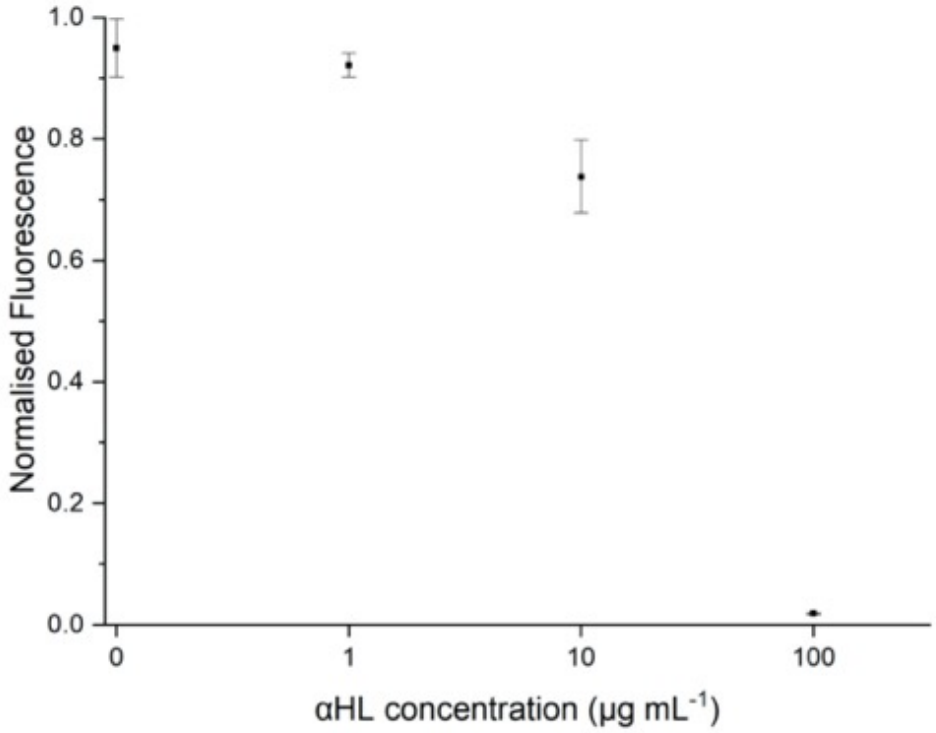
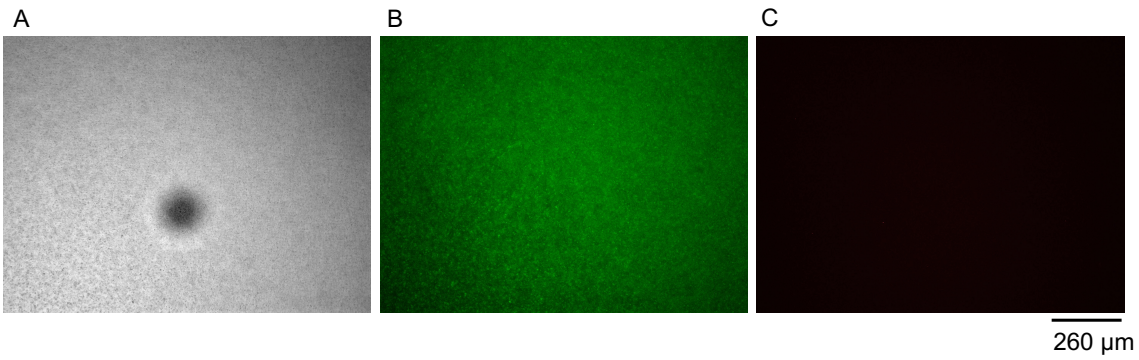


Figure 3.8: Release of the fluorescent molecule NBD-glucose from aqueous droplets into a hydrogel layer can be controlled by variation in αHL concentration. The mean fluorescence of droplets containing 0, 1, 10 & 100 μg/mL αHL was tracked over a 16-hour period and normalised to the fluorescence at the beginning of the experiment. Each point is the mean of 3 technical replicates. Error bars represent the standard deviation.

3.2.5 Gene induction using single L-arabinose-containing droplets

In the next step, we investigated whether single droplets containing L-arabinose could induce gene expression in a layer of bacteria-containing hydrogel. We carried out the experiment in a similar fashion to the NBD-glucose experiments. Optimised from Chapter 2, we formed a hydrogel layer (150-200 μm thick) inside the experimental chamber containing *E. coli* cells with an L-arabinose responsive plasmid. We then added a lipid/oil solution and ejected an M9-based droplet of 180 μm diameter containing 0.5% w/v L-arabinose as well as 0.1 mg/mL αHL optimised from 3.2.4 into the well. The droplets sank to the bottom and formed a DHB leading to the release of L-arabinose into the gel layer. We then incubated the well for 18 hours at 37°C and subsequently investigated mCherry expression using fluorescence imaging. In these conditions, we observed no mCherry expression after overnight growth (Fig. 3.9 C, D). Expression of GFP confirmed healthy growth of the bacterial strain (Fig. 3.9 B).



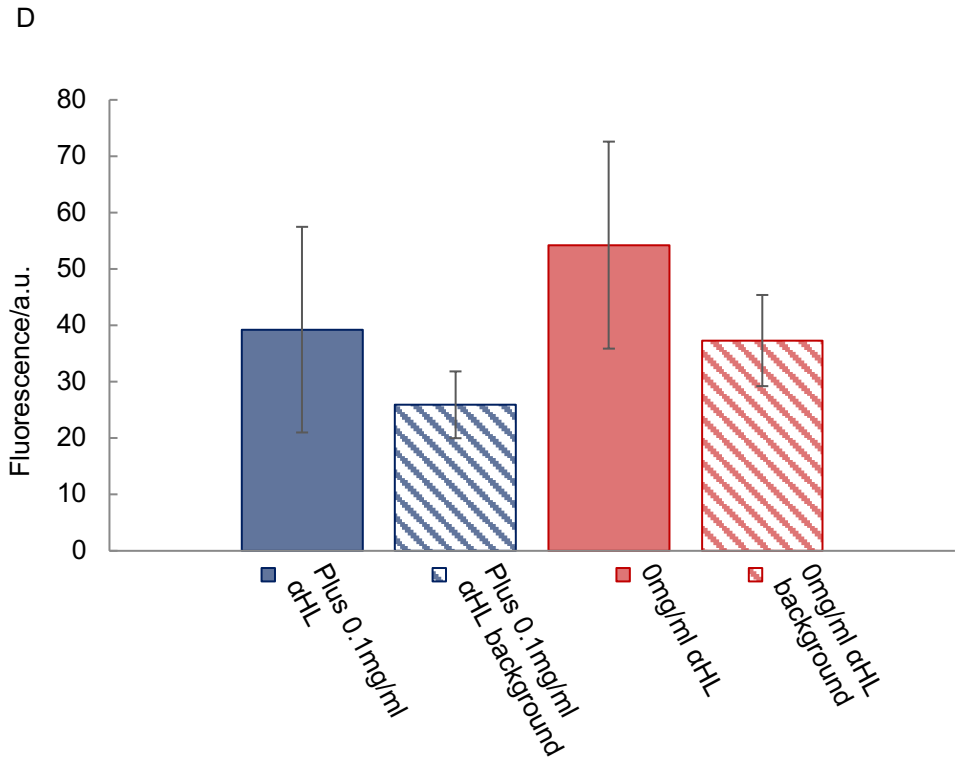


Figure 3.9: Release of the inducer L-arabinose from single droplets (180 µm diameter) into a bacteria-containing hydrogel. Images were taken 18 hours after addition of droplets onto the hydrogel. Three representative microscopy images are shown in the top row. The brightfield channel shows a single aqueous droplet sitting on top of a hydrogel containing bacteria (A). The green fluorescence channel shows a uniform distribution of E. coli cells throughout the gel (B). The red fluorescence channel shows no expression of mCherry suggesting that no gene induction had occurred (C). The mean mCherry expression was quantified in the gel layer in close proximity to the droplet and in an area at the edge of the well to examine background

fluorescence (D). The experimental group shown in blue contained 0.1 mg/mL αHL. The control group shown in red did not contain αHL. Each point is the mean of 3 technical replicates. Error bars represent the standard deviation. A t-test was carried out to confirm that there was no statistically significant difference in mCherry induction between droplets containing the protein pore and the control group (p= 0.4706, t = 0.7961, t = 1.558, df = 4).

One possible explanation for these results is that the cells within the hydrogel had not been exposed to a high enough concentration of inducer, or that the time of exposure was too short. The concentration of the inducer next to the droplet was likely close to 0.5% w/v when it first formed a DHB. Dye diffusion of NBD-glucose (see section 3.2.4) indicates, however, that this concentration will likely drop rapidly within the first 45 minutes as the inducer diffuses into the hydrogel. From Chapter 2 (Fig. 2.7), it can be concluded that induction occurs at a concentration of 0.05% w/v, 10x lower than the concentration in the droplets used here. This indicates that the most likely explanation for not observing mCherry expression is that the cells were not exposed to the inducer for a long enough periods of time. As described in the previous chapter L-arabinose induction requires the expression of L-arabinose transporters that start the positive feedback loop (Fig. 2.1). Rapid release of L-arabinose into the hydrogel by single droplets is too fast for this process to take place.

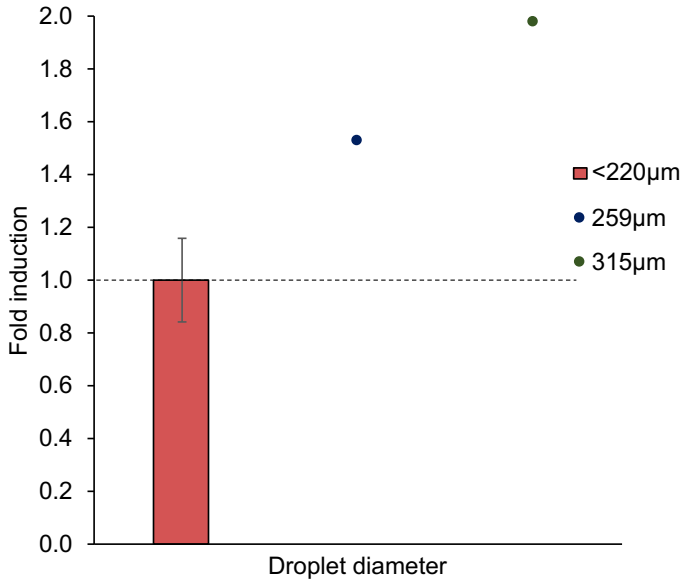


Figure 3.10: Fold induction of mCherry during an 18-hour period following the addition of inducer-containing aqueous droplets of various volumes. Droplets of a diameter of below 220 μm did not result in mCherry expression. Droplets of a diameter of over 200 μm had a decreased half-life. 1 out of 3 droplets of 260 μm and 315 μm diameter remained stable over the 18-hour incubation period. mCherry fold induction from these single replicates is shown in blue and green.

One way to overcome this challenge is to increase the L-arabinose concentration within the droplets. This did however lead to a dramatic decrease in droplet stability due to a greater build-up of osmotic pressure acting on the system. When we repeated this experiment at concentrations above 0.5% w/v L-arabinose, droplets did not survive past the 4-hour mark on top of a hydrogel.

The second solution to this challenge was to increase the diameter of the droplet so a larger payload of arabinose was delivered. We tested a range of droplet diameters (Fig. 3.10). Additionally, we decreased the αHL concentration to 50 μg/mL to further increase droplet stability. We increased droplet sizes from 220 μm – 315 μm. Only

droplets of diameter sizes of ~260 µm & ~315 µm, demonstrated localised mCherry expression. Cells in the area in close proximity to the droplets showed a fluorescence intensity fold induction of up to 2 when compared to the background fluorescence (Fig. 3.11). However, all droplets above 180 µm diameters were not stable and often ruptured after several hours, with only 25% of the 315 µm droplets surviving past the 4-hour mark.

In general, DIBs remain stable at droplet sizes of up to 75 nL. DHBs tend to exhibit a lower degree of stability. pL sized droplets with a diameter of up to 220 µm remained stable over the 18-hour timeframe of the experiment. Larger sized droplets are more susceptible to fusion with the hydrogel layer resulting in a dramatically reduced DHB half-life. However, other factors such as lipid composition, oil composition, humidity and osmotic differences between the droplet and the hydrogel have been shown to influence DHB stability (Booth et. al, 2017).

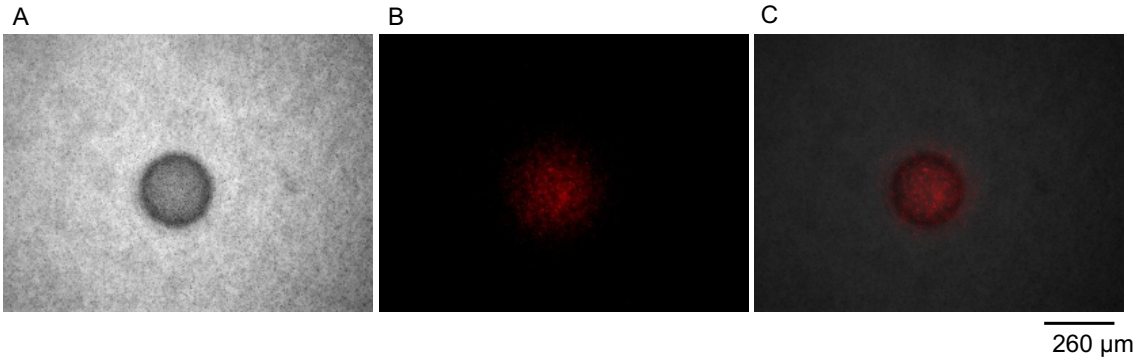


Figure 3.11: Microscopy images showing localised mCherry expression in proximity to an inducer containing droplet after 18-hours of incubation at 37°C. The brightfield image showed an aqueous droplet of a diameter of 260 µm sitting on top of a bacteria-containing hydrogel (A). The red fluorescence channel showed mCherry expression in proximity to the droplet (B). Overlying the two channels showed the localised nature of the gene induction observed in these conditions (C).

These results showed that localised gene expression can be achieved with the single droplet systems. The concentration of inducer required is however at the limit of what can be achieved with this kind of system. High droplet sizes are required to deliver a large enough payload for activation gene expression. Droplets of this large size are, however, not stable over the 18-hour timeframe of gene induction experiments - with most rupturing before the payload can be delivered. Droplet stability remained an immense problem that restricts the use of single droplets. In the next chapter, we show that hundreds of much smaller droplets networked by bilayers is a solution for this system.

3.3 Summary

In this chapter we investigated the use of single droplets for localised gene induction in a homogenous population of *E. coli*. We examined the stability and contact angle of droplet hydrogel bilayers at varying compositions of the oil solution. We found the φ_{SIL} of 0.50 to be an optimal compromise between droplet stability and maximising protein pore insertion. We used the fluorescent dye NBD-glucose as a model to show the diffusion of a small molecule from aqueous droplets into hydrogel layers. We investigated the negative effect on protein pore insertion of a prolonged incubation of single droplets in the lipid/oil solution before DIB formation. We then showed that the concentration of the protein pore αHL can be used to modulate the rate of release of the fluorescent dye. In the last part of the chapter, we achieved localised gene expression using droplets of diameters of over 260 μm containing the inducer L-arabinose. Droplets with lower volumes did not induce mCherry expression. Droplet stability at these larger volumes remained a major issue.

3.4 Materials & Methods

3.4.1 DIB formation and dye diffusion experiments

Aqueous droplets were formed using 10 mM Tris-HCl buffer (Invitrogen) (pH = 8) or M9 medium as described in previous chapters. 2-Deoxy-2-[(7-nitro-2,1,3-benzoxadiazol-4- yl)amino]-D-glucose (NBD-glucose) (Sigma-Aldrich) was dissolved in 10 mM Tris-HCl buffer (pH = 8) to a concentration of 1.45 mM and stored at -20°C for later use. Before the start of dye diffusion experiments, the stock solution was diluted in Tris-HCl buffer or M9 medium to a final concentration of 100 μM. Monomeric αHL from *Staphylococcus aureus* was obtained from our group and unless otherwise stated diluted to a working concentration of 100 μg/mL. Aqueous droplets of 75 nL volume were formed using a 0.5 μl glass syringe (Hamilton) in 16-well chambers containing 5.9 mM 1,2-diphytanoyl-sn-glycero-3-phosphocholine (4ME 16:0 PC (DPhPC)). One dye-containing droplet and one buffer droplet were ejected into each well. DIBs were formed immediately by tilting the 16-well incubation chamber leading to the two droplets in each well to come together. During the investigation of the incubation time effect, droplets were incubated for 30 minutes before DIBs were formed.

3.4.2 The effect of oil phase composition on bilayer size and stability

Hydrogel layers were formed as shown in previous chapters. Lipid films of 1,2-diphytanoyl-sn-glycero-3-phosphocholine (4ME 16:0 PC (DPhPC)) were dissolved in undecane (Sigma-Aldrich) and Silicone Oil AR20 at 1:3, 1:1 and 3:1 volume ratios to a final lipid concentration of 5.9 mM DPhPC. 150 μL of these solutions was added to the chamber containing the hydrogel. pL-sized droplets with a diameter of 180 μm containing 100 μM NBD-glucose were ejected directly into the well using a

microinjector (FemtoJet 4x, Eppendorf) with a corresponding microinjector capillary (Femtotip II, Eppendorf). Droplets were imaged over an 18-hour period using a Leica DMi 8 epi-fluorescence microscope. Equilibrium contact angles were measured after an incubation time of 20 minutes according to the method first described in past work from our group (Alcinesio et al., 2020).

3.4.3 Release of L-arabinose from single droplets

The experimental setup was prepared as described above. M9-based aqueous droplets containing 0.5% w/v filter-sterilized L-arabinose as well as 50/100 μg/mL of monomeric αHL were ejected into the experimental well and incubated at 37°C for an 18-hour period. mCherry expression was examined using epifluorescence imaging and quantified using Fiji (ImageJ). The mean fluorescence intensity was analysed under the droplet and on the edge of the well to determine the background fluorescence. Settings were kept consistent between experiments.

4 Patterned gene induction using printed droplet networks

4.1 Introduction

In the last chapter we demonstrated localised gene induction in a homogenous layer of *E. coli* cells using single droplets. However, the poor stability of these nL-sized droplets meant most ruptured before induction could happen. In this chapter we present the solution to this problem of stability using 3D-printed droplet networks. These printed networks comprise of hundreds of pL-sized droplets interfaced by bilayers. In this chapter we explore the process of interfacing droplet networks with bacterial cells: First, we examine the stability of printed droplet networks on top of hydrogels embedded with *E. coli*. Secondly, we investigated the induction of mCherry using droplet networks and required conditions needed for localised gene induction. Finally, we show how patterned droplet networks achieve patterned gene expression profiles in a homogenous populations of *E .coli*.

4.2 Results and Discussion

4.2.1 Introduction to the printing process

Droplet networks are printed using a piezo-driven 3D printer previously developed in our group (Villar et. al 2013). The movement of the nozzle of the printer and thus the final geometry of the droplet network is determined by a software-controlled micromanipulator.

Droplet networks have several advantages to single droplet systems. First, due to the small volume and tight packing of 3D-printed droplets, that make up the overall structure of droplet networks, the lifetime (several weeks) of such structures far exceeds that of single nL-sized droplets (Villar et. al 2013). This property is particularly important when interfacing living cells with aqueous droplets. Future potential applications of this technology in long-term biological processes such as wound healing or the augmentation of damaged organs require systems that are stable over several weeks.

Second, the arrangement of hundreds of pL-sized droplets in the networks can be precisely controlled. This precise spatial control over the structure of droplet networks has been previously used in our group to produce organoids. Here, the printed droplets contained human cerebral cortex cells and were arranged in precise structures used to examine developmental processes (Zhou et. al, 2020).

In the work shown here control over the arrangement of droplets allows for patterning of gene induction. By printing areas of the network that do release the inducer while others do not, we can spatially control mCherry expression in the bacteria-containing hydrogel.

Printing droplet networks is a well-established technique in our group. Coincubating synthetic tissues with a hydrogel containing bacterial cells has, however, not yet been achieved. The ideal arrangement of our experimental setup is shown in Figure 4.1. The illustration depicts the middle of an experimental chamber: a droplet network containing αHL and the inducer L-arabinose is placed on top of a hydrogel containing bacterial cells. The hydrogel is submerged in a lipid/oil solution. During the printing process droplets are ejected one at a time. Once a first layer consisting of 8 x 7 droplets in the *x*, *y* – dimensions is formed a second layer is printed on top of this structure. This continues until the desired number of layers is printed (Fig. 4.5)

4.2.2 Constructing compact droplet networks in our experimental chamber

We investigated two ways of constructing droplet networks. In a first step we tested printing droplet networks directly onto the hydrogel. We prepared the hydrogel in the experimental chamber as described in chapter 2. Due to the hydrophilic surface of the chamber, the hydrogel layer was not perfectly flat and became thicker towards the edge of the chamber. This was due to the hydrogel spreading along the hydrophilic walls of the cuvette (capillary action). When the hydrogel was then cooled, the resulting shape was concave with a flat area in the middle of the well (Fig 2.8 E, in chapter 2).

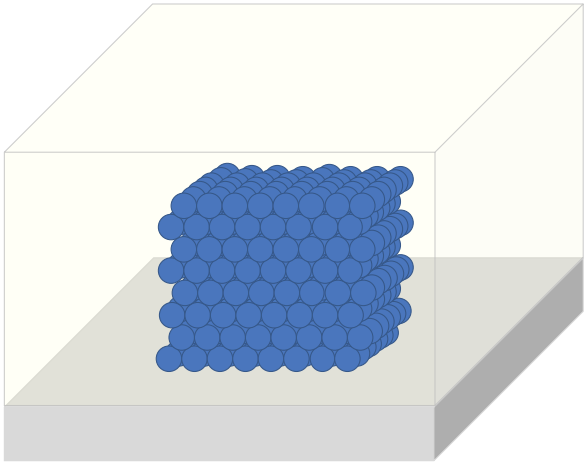


Figure 4.1: A diagram depicting a droplet network (shown in blue) placed on top of a hydrogel containing bacterial cells (shown in grey). The experimental chamber is filled with a lipid/oil solution (shown in beige).

When we first attempted to print directly onto the hydrogel, individual droplets slightly moved during the printing process. They migrated to the middle of the well, the lowest point of the hydrogel. This resulted in disordered structures with droplets not being tightly packed (Fig. 4.2 B). Parts of such structures coalesced into bigger large droplets leading to a poor stability of the overall network. We did not pursue this methodology further has we required compact and stable networks over several hours.

Secondly, we printed droplet networks into a separate container and then transferred the networks consisting of 8 layers of 7 x 8 droplets per layer onto the hydrogel. The flat structure of the printing container preventing any movement of droplets during the printing process. This enabled us to print networks with an exact arrangement of

droplets, without any gaps in the structure. The resulting networks were compact in shape with a tight packing of droplets (Fig. 4.2 A). The structures remained stable over several days.

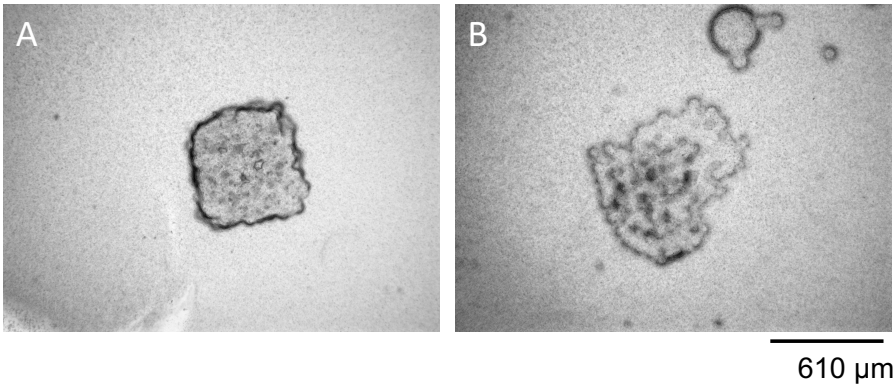


Figure 4.2: Microscopy images showing droplet networks consisting of 7 x 8 droplets per layer with a total of 8 layers. The networks were imaged directly after the printing process from a top view. Networks were either printed into a glass cuvette and then transferred onto the hydrogel (A) or printed directly onto the hydrogel layer (B).

4.2.3 Investigating the structure of printed networks after an 18-hour incubation period

To look at the structure of droplet networks in more detail, we printed networks containing the fluorescent dye calcein and transferred them onto the hydrogel. Imaging the top layer of the hydrogel suggested that the droplet network was in direct contact with the hydrogel. (Fig. 4.3 C).

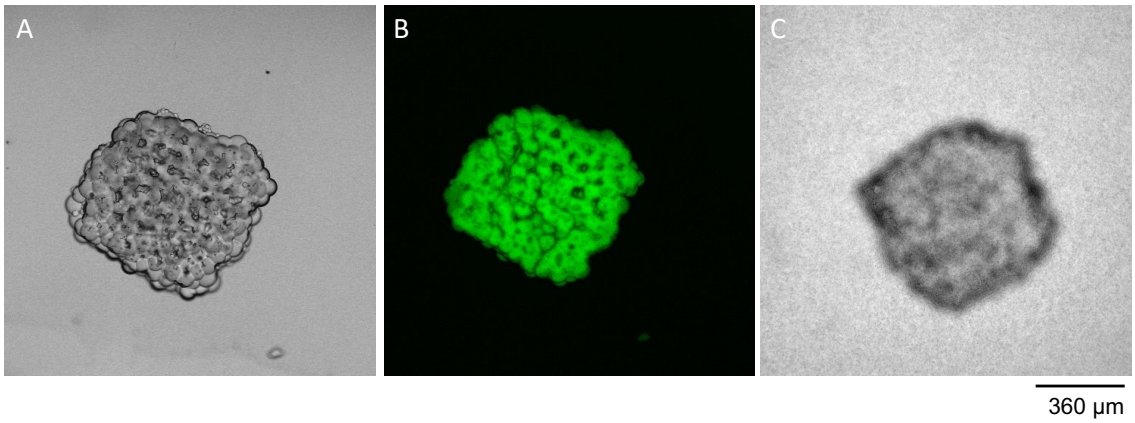


Figure 4.3: Microscopy images of a representative droplet networks placed on top of a hydrogel layer exhibiting tight packing. Brightfield images revealed the exact structure of the bottom layer of droplets that formed a bilayer with the hydrogel (A). Fluorescence images showed the position of individual droplets containing the fluorescent dye calcein (B). When the plane of focus was shifted to the top layer of cells in the hydrogel using an epifluorescence microscope, individual colonies were revealed. The outlines of the networks were observed in the background slightly out of focus suggesting a μm distance between droplet networks and bacterial colonies (C).

Coalescence of individual droplets with the hydrogel layer would lead to the uncontrolled release of the inducer. We confirmed that the structure of droplet networks on the hydrogel remained stable by imaging them over the 18-hour timeframe of the experiment (Fig. 4.4).

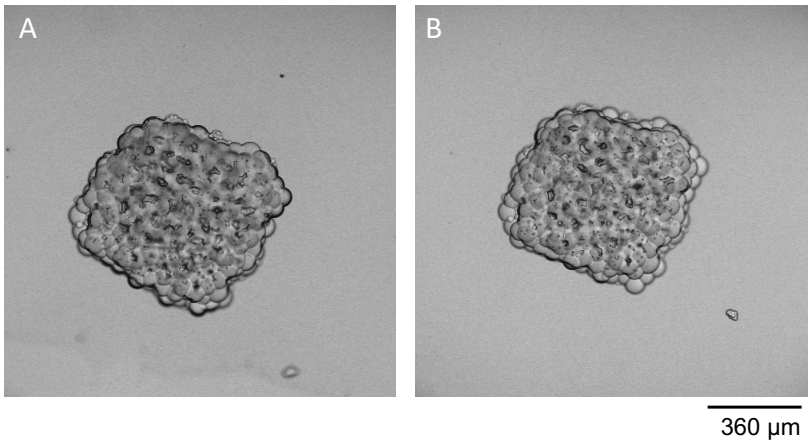


Figure 4.4: Confocal images of droplet networks placed on a hydrogel layer were taken every 30 minutes over an 18-hour period to track each droplet in the bottom layer of the network. Images at t = 0 (A) and t = 18 (B) are shown here. No coalescence of droplets in the network with the hydrogel layer was observed over this period.

4.2.4 Localised induction of mCherry using droplet networks of varying volumes

In the following experiments we investigated localised gene induction using droplet networks. We printed droplet networks containing the inducer L-arabinose & the protein pore αHL. We transferred the networks onto bacteria-containing hydrogel layer as described in section 4.2.2.

We used the variation in the number of layers to investigate how the volume of the droplet network impacts gene induction. When we incubated networks consisting of two, four or six layers of droplets with bacterial cells, minimal gene induction was observed (Fig. 4.5 A, B, C). Networks consisting of 8 layers of droplets, on the other hand, induced mCherry expression (Fig. 4.5 D). Interestingly we observed a clear localisation of mCherry expression in the cells directly below the network. Networks consisting of 10 layers showed a similar area of gene induction. However, in this case we observed an increased background fluorescence, suggesting that the rate of release of the inducer was faster than its subsequent uptake by the *E. coli* cells (Fig. 4.5 E). An 8-layered network with 0.5% w/v L-arabinose contains 1.7×10^{-11} mol of the inducer.

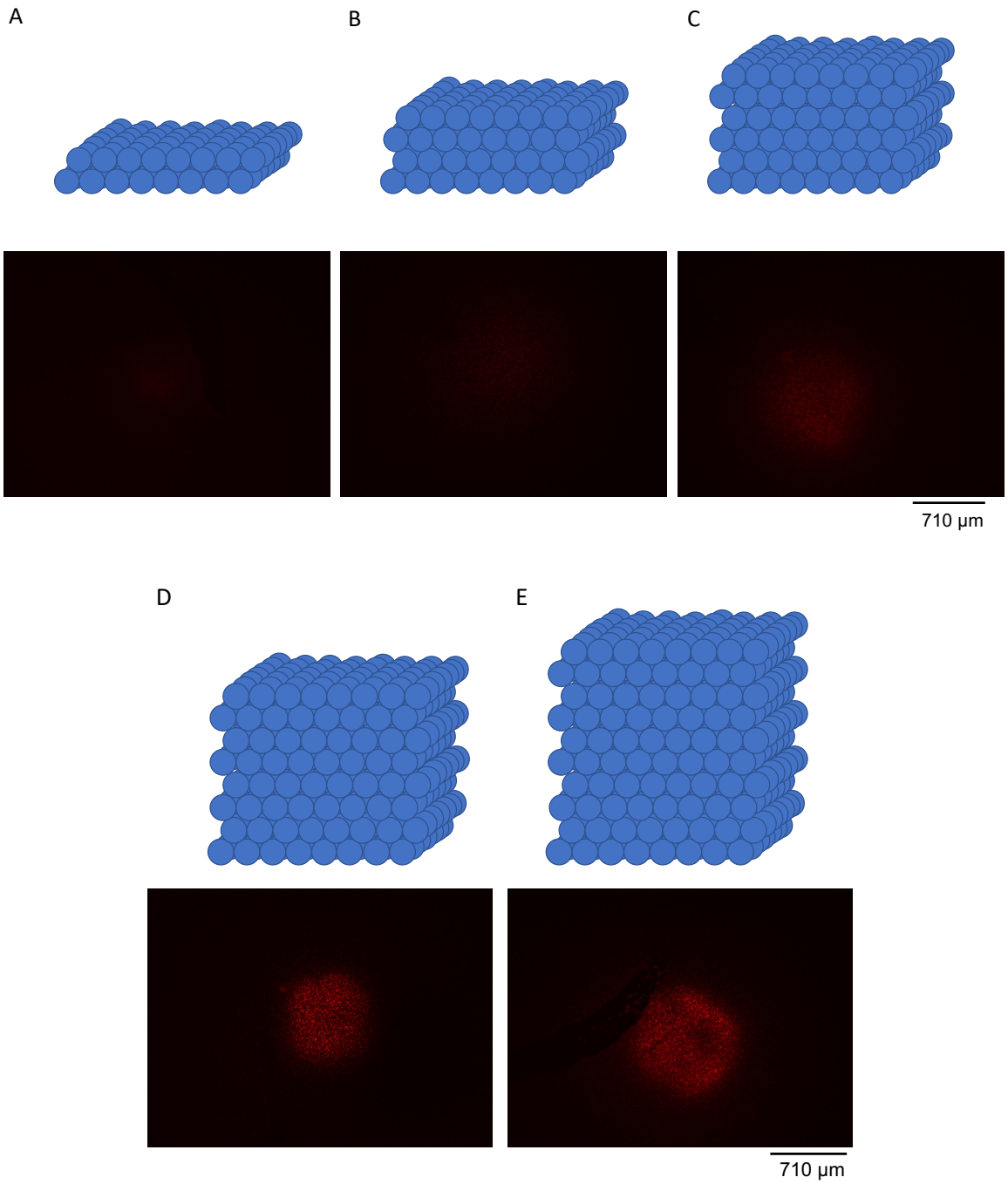


Figure 4.5: Induction of mCherry in *E. coli* cells after 18-hours of co-incubation with droplet networks made up of 2, 4, 6, 8 &10 layers of 7 x 8 droplets. Networks contained 0.5% w/v L-arabinose and 50 μg/mL αHL. A visual representation of the network structure is shown in blue for each condition. mCherry induction was measured using epifluorescence microscopy.

During quantification of the results, we observed a sharp increase in gene induction resulting from 6 & 8 layered networks. Below this volume of the network mCherry expression remained low (Fig. 4.6).

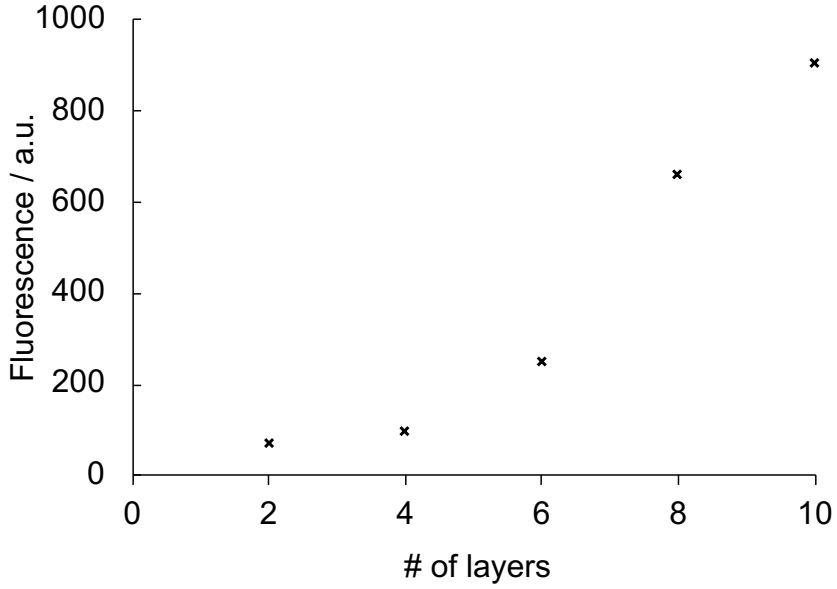


Figure 4.6: Quantification of the induction of mCherry as a result of co-incubation with droplet networks consisting of 2, 4, 6, 8, & 10 layers of 7 x 8 droplets. The mean fluorescence in the area of the gel directly underneath droplet networks was measured using an epifluorescence microscope. Each data point shown is the result of a single technical replicate after the subtraction of background fluorescence.

Here, we show one representative example of gene induction using droplet networks (Fig. 4.7). An important aspect of this is pattern fidelity which we determined using an overlay of the brightfield and red fluorescence channel (Fig. 4.8). The resulting mCherry expression pattern in the hydrogel closely resembles the shape and position of the droplet network above. This high pattern fidelity suggests that the rate of release of the inducer from the droplet network equalled its uptake by the bacterial

cells in the hydrogel. No excess inducer diffused away from the network into other areas of the gel at high enough concentrations to induce mCherry expression.

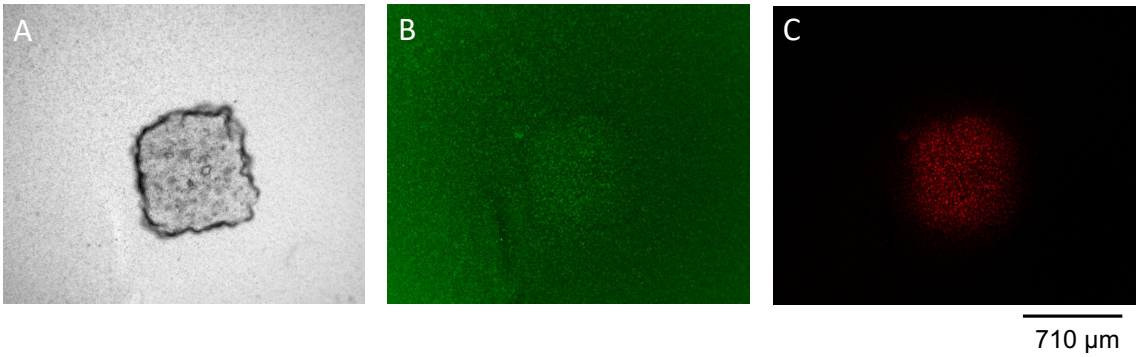


Figure 4.7: Imaging of a representative example of localised gene expression using droplet networks. The brightfield image revealed the position of the droplet network on the gel (A). The green fluorescence channel measured the constitutive expression of sfGFP by the bacterial cells showed a uniform distribution of bacterial colonies (B). The red fluorescence channel revealed a localised gene expression pattern of mCherry.

In areas in close proximity to the network the concentration of L-arabinose was kept at a high enough level for a sufficient period of time to induce mCherry expression. This can be compared to previous results where the quick release of a similar concentration of the inducer for a short period of time using single droplets did not result in induction of mCherry expression (See chapter 3, Fig. 3.9)

Droplet networks used here consisted of 448 droplet that were each separated by a bilayer. We hypothesise that compartmentalisation is crucial to achieve a slow release of a compound over an extended period of time. L-arabinose in the top layer of the network must cross 8 bilayers, the rate limiting step in this process, before it is released into the hydrogel.

In a large single droplet of similar volume and αHL concentration, convection inside the droplet distributes the compound uniformly. We confirmed this hypothesis during the dye release experiments in the previous chapter, where we observed a uniform

decrease in fluorescence intensity thorough the diameter of the droplet (Fig. 3.7). This drastically decreases the required time for the complete release of the compound. We carried out additional experiments to further support this hypothesis later in this chapter (Fig. 4.10).

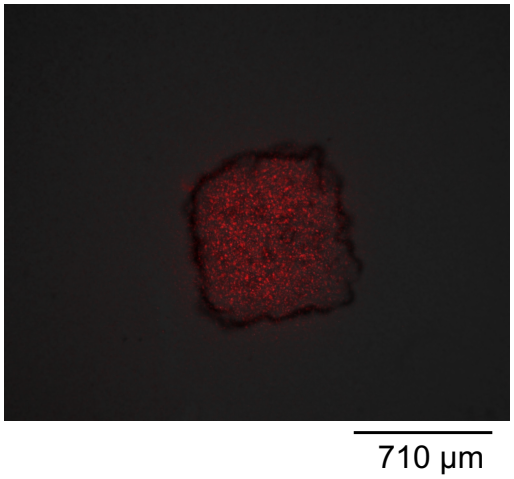


Figure 4.8: Microscopy images showing pattern fidelity of mCherry induction with a droplet network. An overlay of the brightfield and red fluorescence image from Fig. 4.6 revealed a high degree of localisation of gene induction. The shape and position of mCherry induction in the gel layer corresponded precisely to the position of the droplet network.

4.2.5 Release of the inducer from the droplet network can be controlled by the protein pore αHL

An important aspect of the project is the controlled release of the inducer L-arabinose through the αHL pore. This is particularly important when considering future applications of this technology in a clinical setting.

There are two main requirements for the controlled release of the inducer: First, the small molecule must not be membrane permeable in the absence of a protein pore. Second, the molecule must be of the right size to pass though the protein pore αHL after it inserts into a bilayer.

We tested the membrane permeability of L-arabinose in the absence of αHL and the release of the inducer through the pore in the experiment shown below (Fig. 4.9). We transferred networks containing the inducer L-arabinose and the protein pore αHL onto a hydrogel with bacteria. The control group contained the inducer but did not contain the protein pore. We measured the expression of mCherry in the gel after an 18-hour incubation period in the area underneath the networks as well as on the edge of the gel to investigate pattern localisation.

As seen in previous results, droplet networks containing the inducer and the protein pore did induce gene expression with a mean fluorescence of 441 (± 41a.u.) (Fig. 4.9). In the absence of the protein pore, however, we observed no significant increase in fluorescence compared to the background signal. Variance between repeats in the group was slightly increased compared to the background condition, suggesting some minimal leakage of the inducer from the network into the gel layer in the absence of the protein pore. Overall, these results indicate that the inducer L-arabinose did not cross a lipid membrane (consisting of 2 mM DPhPC and POPC at a 2:1 molar ratio) at high enough quantities to induce gene expression in the absence of the protein pore αHL.

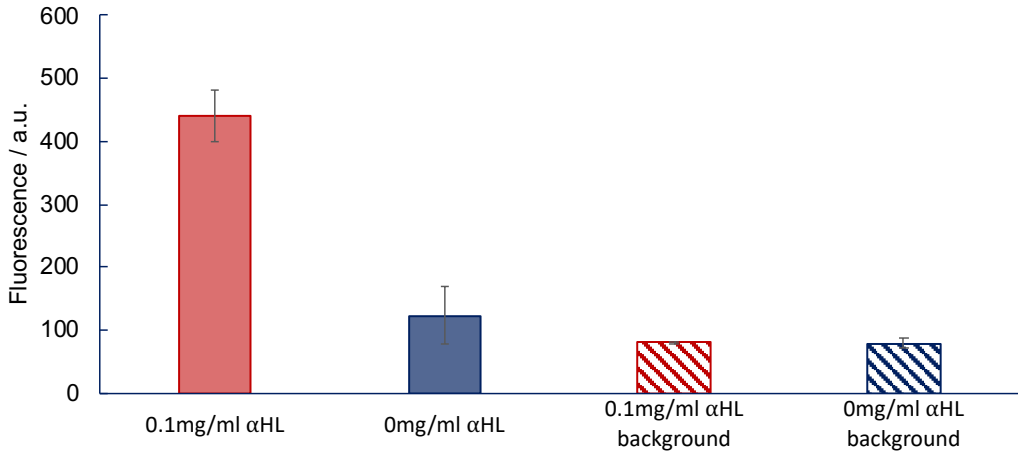


Figure 4.9 Release of L-arabinose from droplet networks through the protein pore αHL. Droplet networks containing the inducer L-arabinose and the protein pore αHL

(shown in red) resulted in localised mCherry expression after 18-hours of co-incubation. Networks containing L-arabinose without the protein pore αHL (shown in blue) did not significantly increase mCherry expression in proximity to the droplet network when compared to the background fluorescence. Each point is the mean of 3 technical replicates. Error bars represent the standard deviation. Results indicated no significant difference in mCherry expression between the control group and the experimental group. A t-test was performed to statistically confirm this result ($p=0.2075$, $t = 1.5021$, $df = 4$).

4.2.6 A slow release of the inducer is required to activate gene expression in the bacterial strain

Droplet network used here consists of 448 droplets of 0.5% w/v L-arabinose. If this amount of inducer is released into the hydrogel steadily via a droplet network, we observed a localised pattern of mCherry expression.

In the following experiment we tested the effect on gene induction of releasing the same volume of inducer onto the gel layer all at once. To do this, we printed 448 droplets into an oil-solution that did not contain any lipid. In the absence of lipid, no monolayer forms around each aqueous droplet when printed, leading all droplets to coalesce into one big droplet. We then added this droplet directly onto a hydrogel which resulted in it instantly fusing with the gel. We compared this instant release of inducer with a control group where we did not add any inducer to the gel at all.

Results indicated no significant difference in mCherry expression between the control group and the experimental group (Fig. 4.10). In both groups mean fluorescence values ranged around 90 a.u. These values are comparable to the background fluorescence in previous experiments (Fig. 4.9). As a comparison, in the area of L-arabinose release directly below the droplet network, fluorescence values range around a mean fluorescence of 441 (± 41a.u.) (Fig. 4.9).

These results underline the importance of a slow release of the inducer, resulting in an elevated local concentration of L-arabinose in the hydrogel layer underneath the droplet network. We estimate this concentration to be close to the 0.5% w/v of inducer inside droplet networks at the beginning of the experiment. When the inducer is released into the hydrogel all at once it rapidly diffuses throughout the gel and reaches an overall equilibrium concentration that is too low to activate gene induction.

The volume of inducer that we added in this experiment consisted of 448 droplets (60 μm diameter) and an inducer concentration of 0.5% w/v. When this volume of inducer is equally distributed throughout the 120 μL gel the inducer will be diluted around 1500 times resulting in an L-arabinose concentration of $3x10^{-4}$ %. This concentration is 3 order of magnitudes lower than the local concentration reached in the hydrogel underneath a droplet network (0.5% w/v). This simple calculation helps to understand the importance of a slow, controlled release of a small molecule via droplet networks.

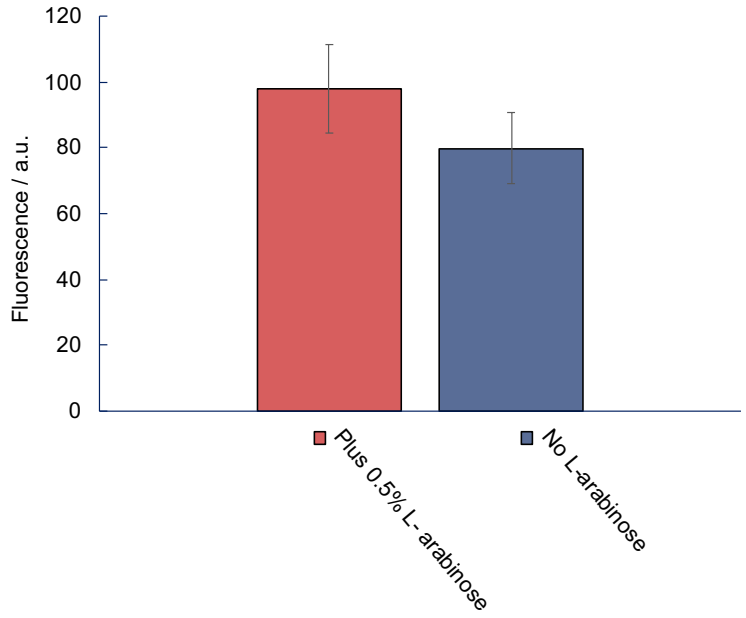


Figure 4.10: mCherry induction in a hydrogel following the rapid release of L-arabinose. The volume of inducer added was set at the volume of an 8-layered

droplet network used in previous experiments. No inducer was added to the control group. Mean fluorescence was measured 18 hours after addition of the inducer. Each point is the mean of 3 technical replicates. Error bars represent the standard deviation. A t-test was performed to statistically confirm that the level of mCherry induction in the experimental and control group where not statistically significant ($p=0.1636$, $t = 1.7038$, $df = 4$).

4.2.7 Localised gene induction requires the uptake and metabolism of the inducer by the bacterial cells

A local pattern of gene expression can only be achieved if the release of the inducer from the droplet network matches its uptake by the bacterial cells. If the inducer is not taken up and contained within the cells at sufficient quantities, it will diffuse throughout the gel and any localisation effect is lost.

In the following experiments we used the membrane permeable nucleic acid stain Syto-9 to illustrate this point. We added a single droplet containing the stain onto a gel layer with bacterial cells. In the beginning of the experiment cells in close proximity to the droplet were stained (Fig. 4.11 A). Over a 15-minute period the dye diffused to a large area of the gel which resulted in the loss of any localised effect (Fig. 4.11 E). This contrasts with the inducer L-arabinose used in previous experiments which is taken up and metabolised by *E. coli* colonies in the hydrogel (Desai et. al, 2010). The inducer is only present underneath the network and does not diffuse into other areas of the gel at high enough quantities to induce gene expression (Fig. 4.8).

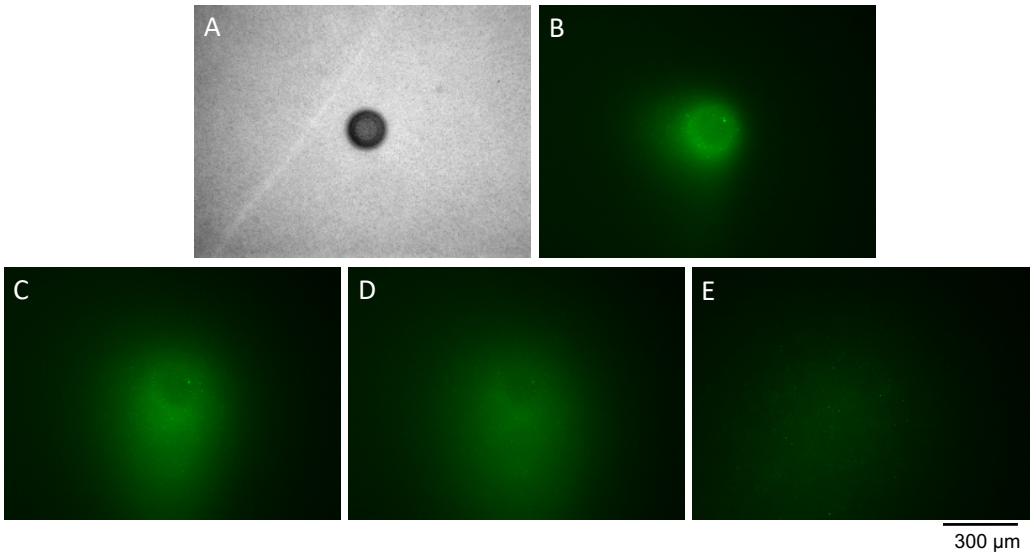


Figure 4.11: Microscopy images showing no localised effect when releasing the nucleic acid stain Syto-9. The dye diffused out of a 140 μm sized droplet (A). Staining was observed in proximity to the droplet after 30 seconds (B). Localisation of the effect is lost over time. Images were taken after 3 minutes (C), 5 minutes (D) and 15 minutes (E). Images shown here are representative of 5 technical replicates.

4.2.8 Balancing the release of the inducer from a network with its uptake by the bacterial cells

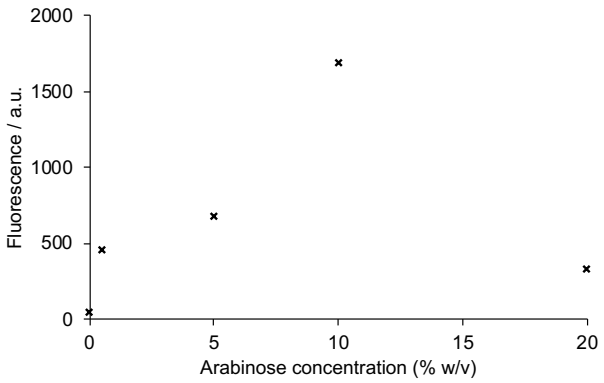
There are several factors that can be modulated to balance inducer release from droplet networks and inducer uptake by bacterial cells. We can alter the concentration of the protein pore within the network, changing the permeability of bilayers within the network (see Fig. 3.8). Additionally, we can adjust the cell density within the hydrogel. At a high colony density, more L-arabinose can be taken up and metabolised by the cells within the hydrogel. There is, of course, an upper limit to the cell density within a hydrogel. At a low colony density, a minimal amount of inducer will be consumed by the cells. When seeding cells too thin, the overall intensity of mCherry expression will decrease, making gene induction patterns harder to detect.

A factor in the system that can be easily adjusted is the concentration of L-arabinose within droplet networks. In the following experiment we printed droplet networks with varying concentrations of L-arabinose ranging from 0-20% w/v. We then measured the expression of mCherry in the area underneath the droplet network and compared the results between conditions (Fig. 4.12 A).

Gene induction increased up to an L-arabinose concentration of 10% w/v. At concentrations over 0.5% w/v, however, we observed a decrease in pattern fidelity suggesting that more arabinose was released from droplet networks than could be taken up by the bacterial colonies. We investigated this loss in pattern fidelity at high L-arabinose concentrations in follow up experiments later in the chapter (Fig. 4.15).

At an L-arabinose concentration of 20% w/v mCherry expression decreased due to a loss in network stability (Fig. 4.12 B). Osmotic imbalance from the high concentration of inducer led to coalescence of droplets within the network and fast release of the inducer into the gel. As shown earlier in the chapter rapid release of inducer does not lead to mCherry induction (Fig. 4.10).

A



B

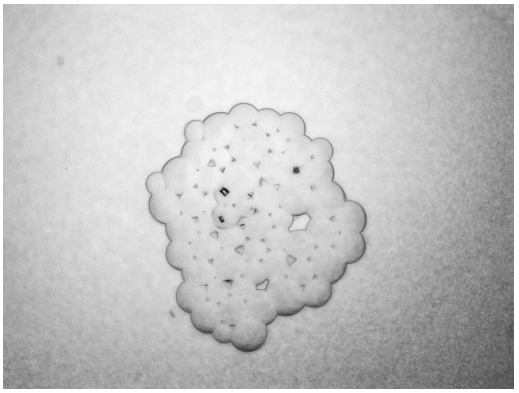


Figure 4.12: Mean mCherry induction by an 8-layered droplet network with 0%, 0.5%, 5%, 10% & 20% w/v L-arabinose after 18 hours of incubation (A). A microscopy image showing the structure of a droplet network containing 20% w/v L-arabinose after the incubation period (B).

4.2.9 Patterned gene induction using droplet networks

One of our major goals of this project was to not only show localised gene expression but to also generate patterned responses. To achieve this, we constructed droplet networks comprising of droplets either containing the inducer L-arabinose and the protein pore αHL (shown in red, Fig. 4.13 A, Fig. 4.14 A) or not containing either (shown in blue, Fig. 4.13 A, Fig. 4.14 A).

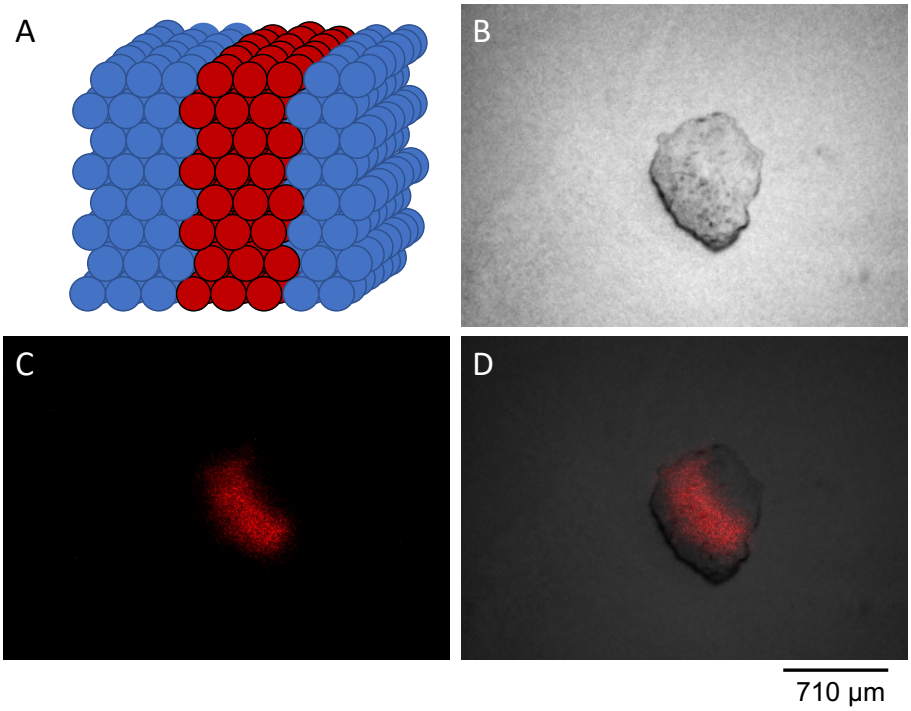


Figure 4.13: Patterned gene induction using droplet networks. A stripe pattern was printed according to the visual representation shown in (A). Red droplets contained 0.5% w/v L-arabinose and the αHL pore. Blue droplets contained M9 buffer. The brightfield images shows the structure of the network after 18 hours of incubation on the hydrogel (B). The red fluorescence channel shows the mCherry expression pattern induced by the droplet network above (C). On overlay of the brightfield and fluorescence images shows a high degree of pattern fidelity (D).

We tested two types of patterns: The first type of network contained one stripe with the inducer in the middle of the structure. The second type of network contained two stripes with the inducer on either side of the structure.

Figure 4.13 shows the resulting mCherry gene expression pattern from droplet networks that contain a single stripe of inducer-filled droplets. From the brightfield image we can conclude that the printed structure is not completely rectangular. These imperfections were caused during the printing process due to imperfect alignment of the two printing nozzles. However, the overall structure of the network was intact and consisted of a single 3-droplet thick stipe surrounded by buffer filled droplets. The red fluorescence image (Fig. 4.13 B) shows the expected gene induction pattern. The area of gene induction stretched across approximately a third of the droplet network and was positioned in its middle (Fig. 4.13 D). These results show that patterned gene expression can be achieved with a high fidelity by producing corresponding droplet networks.

We made the final attempt at patterned gene expression using a 2-stripe pattern (Fig. 4.14). Printing was improved when compared to previous experiments. Careful alignment of the 2 nozzles resulted in an accurate square-shaped network (Fig. 4.14 B). The mCherry expression pattern showed 2 well defined stripes (Fig. 4.14 D).

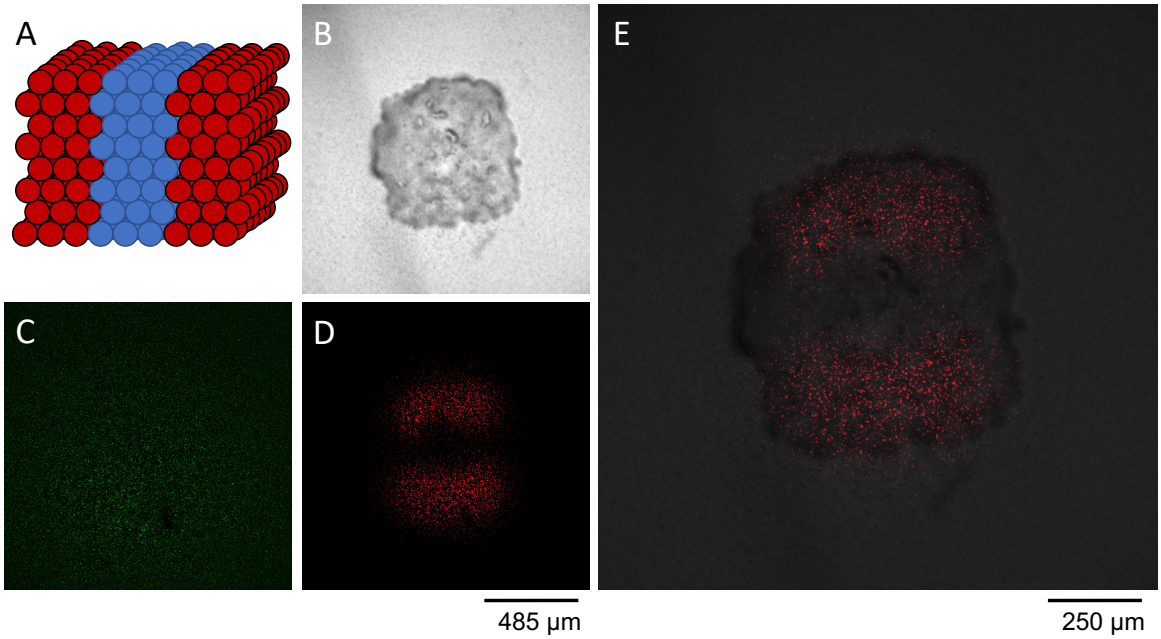


Figure 4.14: Patterned droplet networks consisting of 2 stripes were printed according to the visual representation shown in (A). Red droplets contained 0.5% w/v L-arabinose and the αHL pore. Blue droplets contained M9 buffer. The brightfield images shows the structure of the network after 18 hours of incubation on the hydrogel (B). The green fluorescence channel shows a uniform distribution of bacterial colonies throughout the gel (C). The red fluorescence channel shows the mCherry expression pattern induced by the droplet network above (D). An overlay of the brightfield and fluorescence images shows a high degree of pattern fidelity (E).

4.2.10 Inducer release from patterned droplet networks must be balanced with inducer uptake to maintain high pattern fidelity

To investigate this hypothesis, we printed 2-stripe networks of similar structure as in the previous experiment (Fig. 4.14 A). However, here we increased the L-arabinose concentration from 0.5% to 5% w/v. As expected, the produced pattern showed a much lower pattern fidelity when compared to results from networks with 0.5% w/v L-arabinose - the 2 induced stripes were hardly distinguishable (Fig. 15). This was the result of L-arabinose diffusion from the network into the gel layer at a concentration that exceeded its uptake by the colonies in the gel. Excess inducer then diffused into other areas of the gel inducing gene expression in undesired areas. This experiment

underlined the importance of balancing the three main parameters of the experiment to achieve localised gene induction: L-arabinose concentration, the rate of inducer release and cell density in the hydrogel.

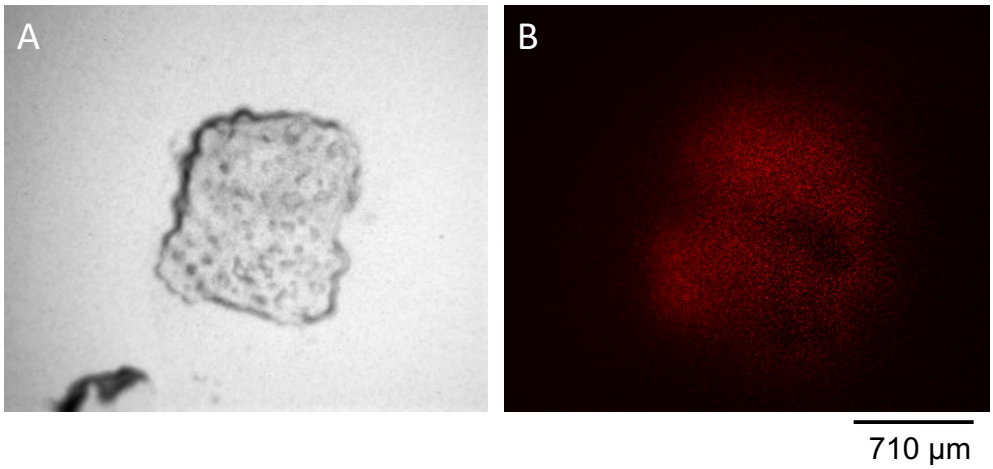


Figure 4.15: Two stripe gene induction using droplet networks containing 5% w/v of L-arabinose. A brightfield image of the droplet network after 18 hours of incubation on a hydrogel shows the intact structure of the network (A). The red fluorescence channel shows the resulting gene induction pattern that was characterised by a low pattern fidelity (B).

4.3 Summary

In the work in this chapter, we showed the first patterned gene induction in a population of bacterial cells using droplet networks. We were able to localise gene expression to the area of the gel adjacent to the droplet network. We generated patterned responses by producing droplet networks that were made up of several stripes with different droplet content. We showed the importance of parameters required to achieve a localised response such as the rate of inducer release by the droplet networks and its uptake by the bacterial colonies. Furthermore, we demonstrated that the inducer has to be permanently taken up and consumed by the bacterial cells to avoid the diffusion of the small molecule into undesired areas of the gel.

4.4 Materials & Methods

4.4.1 Assembly of droplet networks

The printing process was previously described in work from our group (Villar et. al 2013). The system was based on a custom-built printer consisting of a computer controlled and piezo-driven transducer. Aqueous droplets were ejected from a glass nozzle that was mounted onto a micromanipulator. The solution was ejected into a quartz chamber filled with a 2 mM solution of 1,2-diphytanoyl-sn-glycero-3-phosphocholine (4ME 16:0 PC (DPhPC)) and 1-palmitoyl-2-oleoyl-sn-glycero-3-phosphocholine (16:0-18:1 PC (POPC)) at a molar ratio of 2:1. The lipids were prepared as described in previous chapters and dissolved in Silicone Oil AR20 and undecane (Sigma-Aldrich) at a 65:35 volume ratio. Each layer of the printed structures was made up of 7 x 8 droplets (65 μm diameter) arranged in a rectangular shape. Unless otherwise stated networks consisted of 8 layers of droplets. The printing solution was based on M9 medium as described in previous chapters. After completion of the printing process networks were incubated in the quartz chamber for 15 minutes to ensure complete bilayer formation within the structure. Networks were subsequently transferred into the experimental chamber using 20 μL pipette tips. Imaging with fluorescent dyes was performed using 10 μM calcein (Sigma) dissolved in M9 medium.

During gene induction experiments droplet networks contained 50 μg mL^{-1} monomeric αHL pore and 0.5% w/v L-arabinose unless otherwise stated. Patterned droplet networks were printed using 2 nozzles in parallel. The first nozzle was filled with a printing solution containing both the protein pore and the inducer. The second solution contained only buffer. Experimental chambers were incubated for 18 hours at 37°C before imaging.

4.4.2 Manual addition of L-arabinose

448 droplets of M9 medium (the volume normally present in droplet networks) containing 0.5% w/v L-arabinose were printed in an oil solution not containing lipid. All droplets coalesced into one large droplet that was transferred into the experimental well that also contained a lipid-free oil solution. Upon addition of the droplet the solution merged with the gel instantly. The chamber was incubated for 18 hours at 37°C before imaging.

4.4.3 Imaging of the experimental chamber

Epifluorescence imaging was performed as described in previous chapters. Confocal microscopy was carried out using a Leica SP5 confocal microscope. The exposure and gain were kept constant between experiments. Image analysis was performed using Fiji (ImageJ).

4.4.4 Syto-9 experiments

Cell staining experiments were performed using M9-based droplets containing 500 μM Syto-9 (Thermo Fisher). Droplets (140 μm diameter) were made using a microinjector (FemtoJet 4x, Eppendorf) as described in previous chapters. Imaging was performed 0.5, 3, 5 & 15 minutes after addition of the Syto-9 droplet into the experimental well using an epifluorescence microscope.

5 Conclusion & Future Directions

5.1 Conclusion

In this work, we showed that droplet-based systems are a viable option of interacting with biological cells in a locally controlled way.

In the first chapter we investigated the biology behind the L-arabinose inducible plasmid. We established conditions that allowed for optimal growth of our bacterial strain in an experimental setup that would later allow us to co-incubate droplet networks and growing *E. coli* colonies.

In the second chapter we looked at single droplet systems in the context of using them for longer term interactions with biological cells. We showed the controlled release of a fluorescent dye in a DHB setup. Furthermore, we saw that localised induction of gene expression is possible by releasing the inducer L-arabinose from a single droplet. Droplet stability remained a major challenge that hindered the use of single droplets with diameters of over 250 μm. Both the high inducer concentration and the long period of exposure required to activate gene expression in our system are beyond the capabilities of such systems.

In the third chapter, we showed that droplet networks are a suitable alternative to single droplets. Due to the smaller volume of the droplets making up such networks and the tightly packed structures that they form, stability is drastically improved. This allowed us to both experiment with the concentration of the inducer and the overall volume of the droplet network. After optimisation, we showed the first localised induction of gene expression in a hydrogel containing bacterial cells using droplet networks. Gene induction occurred in bacterial cells that were in close proximity to the droplet networks. We then built upon this high degree of pattern fidelity by printing droplet networks with internal stripe patterns that led to corresponding

patterns of gene expression in the hydrogel layer. Furthermore, we investigated the conditions required to achieve a localised gene induction. It became apparent that the correct balance between the rate of release of the inducer from the droplet network and its uptake by the bacterial cells in the hydrogel is essential to achieve spatially controlled gene expression patterns. This hypothesis was then tested by increasing the rate of inducer release from droplet networks which resulted in a loss of pattern fidelity. A further requirement of our system to achieve localised effects is the uptake and consumption of the inducer by bacterial cells. Using a membrane permeable cell stain, we showed that without the ability to keep the molecule within a cell after exposure, pattern fidelity is lost over time as the effector diffuses freely throughout the gel. Overall, this work shows that droplet-based systems and biological cells can be interfaced reliably. Importantly, we showed that these interactions can be spatially defined if the criteria outlined in this work are met. This work opens up new avenues in our field allowing us to explore spatially defined interactions between synthetic tissues and biological cell.

5.2 Applications of the current system

5.2.1 Controlling the competition between two bacterial strains using droplet networks

In our work up to this point, L-arabinose was used to induce the expression of a fluorescent protein downstream of the P_{BAD} promoter. In future work it will be important to show that such systems can be modified to locally express functional genes in an area next to the droplet network. In the system illustrated below a population of two different strains of *E. coli* are grown in the hydrogel at the beginning of the experiment (Fig. 5.1). One of the two strains, in this case the green strain, contains a plasmid with a toxin under the control of the P_{BAD} promoter. The toxin

system can be based on naturally occurring colicin toxins that were extensively used in previous work in our group (Krishna Kumar et al., 2020). The droplet network would induce toxin production in adjacent cells leading to the death of the red strain in this area. The green strain, on the other hand, is resistant to its own toxin and could then outgrow the red strain in the gene induction zone.

By controlling the competition between two bacterial strains we could show that our system can be applied to a real biological phenomenon illustrating the versatility of our current system.

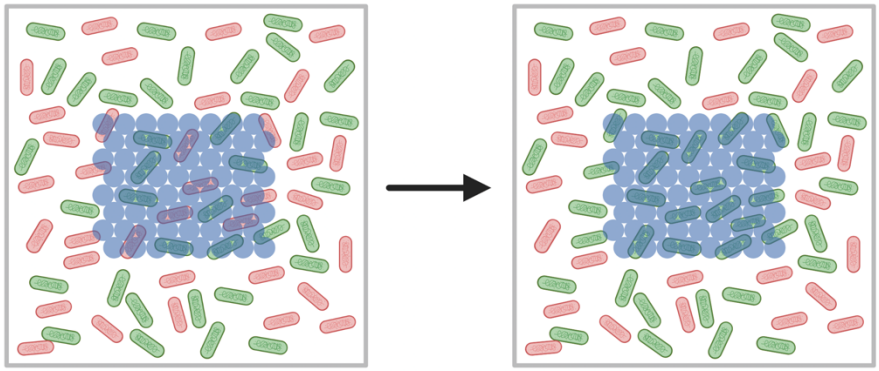


Figure 5.1: A diagram depicting the use of droplet networks to influence the competition between two bacterial strains. The expression of a toxin in the green strain is controlled by the network leading it to outcompete the red strain in the area underneath the droplet network.

5.2.2 Two-way communication between bacterial cells & droplet networks

In our current experiments a signal, in our case the release of an inducer, is passed onto bacterial cells that respond by producing a fluorescent protein. A future improvement of this system could be the incorporation of a two-way communication between droplet networks and bacterial cells (Fig. 5.2 A). This system could be based on simple genetic components in both the bacterial strain and the droplet network. *In vitro* transcription translation (IVTT) systems have been previously

integrated into droplet networks but have not been interfaced with biological cells yet (Booth et. al, 2017). A simple system could consist of a bacterial strain growing inside the hydrogel that produces a quorum sensing molecule once a high enough cell density is reached. This signal then diffuses into the droplet network where it is recognised by its cognate promoter. Production of a downstream gene such as a protein pore leads to the release of a cargo from inside the network into the hydrogel with bacterial cells and closes the two-way communication loop.

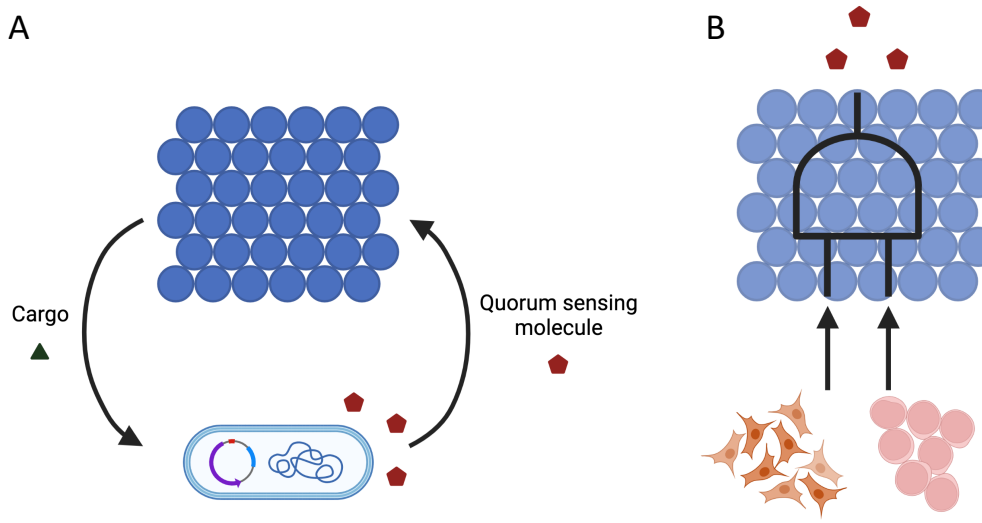


Figure 5.2: A diagram showing potential future use cases of droplet networks. A two-way communication system could detect the presence of a signal from bacterial cells, transcribe & translate an enzyme or protein pore and release a cargo (A). IVTT systems could also be used to encode logic into droplet networks. Two separate biological signals are processed by a droplet network and lead to an output such as cargo release (B).

A further improvement of this system would be the ability to process multiple incoming signals (Fig. 5.2 B). Droplet networks are comprised of hundreds of separate compartments which can help to respond to complex input. Compartmentalisation allows for different areas of the network to carry out different functions. Information on the order of signal processing can be controlled by the

structure of the network and by changing the permeability of bilayers between compartments by incorporating protein pores. Like multicellular organisms where different systems comprised of many cells carry out different functions, one can imagine droplet networks with a similar division of labour. In the future, such systems could be used for therapeutic applications where droplet-based systems sense & process signals from biological cells and respond to disease accordingly.

Mathematical modelling of our system would be a suitable way of further exploring the parameter space of our experimental setup. Diffusion has been extensively modelled in a biological context, including, for example, the effect of diffusion dependent morphogen gradients on gene expression (S.Y. Shvartsman & R.E. Baker, 2012). This could help to assess expected potential gene expression patterns in silico before performing experiments experimentally.

5.2.3 Interfacing droplet networks with mammalian cells

In this project we interfaced droplet networks with bacterial cells. In future projects it will be necessary to show similar results with mammalian cells. We carried out preliminary experiments using droplet networks based on mammalian cell medium and observed a significant reduction in network stability. Furthermore, experimentally working with mammalian cells comes with its own set of difficulties. Conditions such as temperature, CO_2 concentration and humidity must be carefully controlled during the timeframe of the experiment while also accommodating for tight parameters that ensure network stability. These issues can be resolved by altering some of methods used in this work.

The work with mammalian cells would open up new possible applications of droplet networks. Processes such as cell differentiation, cell migration or wound healing

could be influenced using this technology. These processes require special conditions i.e. the presence of a transcription factor that regulate stem cell fate in a locally precise way. Specialised microenvironments or niches play a crucial role in man biological processes like for example haematopoiesis and have been the target of therapeutic approaches in the past (Adams et. al, 2007).

However, the main challenge remains finding a system that enables a local interaction between droplet networks and mammalian cells. The released molecule must be membrane impermeable, in the absence of a protein pore, to enable a tight control over the speed of its release. Additional factors that are discussed in this work are required to achieve localised effects: this includes the permanent uptake or metabolism of the molecule to prevent its diffusion across the gel.

One possible solution to these problems is the use of active transport through membrane proteins as opposed to their passive diffusion through a protein pore. Here, the buffered environment required in mammalian cell medium makes the use of proton pumps difficult. Alternative pumps transporting Ca^{2+} or ATP could be promising candidates.

To achieve more complex functions, it will be required to release proteins and peptides from droplet networks in a controlled way. This would drastically improve the range of applications of droplet networks in areas such as the treatment or replacement of damaged tissues and organs.

One question that remains is role of purely synthetic tissues in this development. The most promising alternative approach is the production of organoids (Schutgens et. al, 2020). These in vitro-cultured structures can be made from the patient's own tissues mitigating the risks of unfavourable immune reactions. We do, however, currently lack tight control over the production of such organoids preventing extensive clinical

applications of such systems. Purely synthetic tissues made up of defined components could aid this process. In particular, hybrid tissues consisting of individual organoids that are interconnected and controlled by droplet-based systems could provide a way towards real life application of this technology.

5.2.4 Towards bioimplantable devices based on droplet networks

Lastly, we will discuss some of the key challenges that remain in the field of droplet networks.

The first issue is droplet stability: droplet networks provide a considerable advantage in this aspect when compared to a single droplet of larger volume. However, synthetic tissues still lack the structural properties of biological tissues. Even after transferring such systems from an oil into an aqueous phase, implantation of current systems would not be possible. Stability of the system relies on the tight control of humidity & osmolarity, preventing mechanical stress and shielding bilayers from molecules that can disturb the membrane. In a clinical setting after implantation all these factors would result in the quick disintegration of droplet networks.

A distinction of potential application of such systems can be drawn between short-lived uses such as the one-off sensing or drug delivery after surgery and long-lived implants.

During short term application, droplet networks could be protected by embedding them into biocompatible hydrogels such as poly-lactic acid (PLA) based materials that are approved for implantation by the FDA (Liu et. al, 2020).

Long term applications will require a change in membrane composition. Potential alternatives to biological membranes are synthetic materials such as block copolymers that can self-assemble into a variety of morphologies such as vesicles (Mai et. al, 2012).

The second key issue is powering droplet networks. In the system used in this work the aqueous phase contains L-arabinose at the beginning of the experiments. The inducer gradually diffuses out of the network until the concentration equilibrates with the gel layer. Currently there is no way of easily refuelling the system. This problem

also prevents longer term applications of droplet networks such as the release of antibacterial agents to aid in wound healing after surgery (Saghazadeh et. al, 2018). Polymyxin B for example is applied to the wound site at a concentration of 10 μM (Avedissian et. al, 2019). At this rate of release an implant based on droplet networks would deplete rapidly.

Although compounds can be made within droplet networks and vesicles, the production eventually halts as essential components run out and waste products accumulate (Elani et. al, 2014). Incorporating biological metabolic pathways into such systems could be a solution to this problem. In the long term, one can imagine a bioimplantable device that is completely powered by the patient's own body.

The third issue is the control over droplet networks. Once implanted, synthetic tissue must fulfil their biological function according to the patients' needs. A previous approach employed in our lab was the external control of droplet networks. This was achieved with UV light and electrical signals (Booth et. al, 2017). An alternative approach is to incorporate sensing within droplet networks (Fig. 5.2 B). Synthetic tissues will then no longer be controlled by the experimentalist but will process biological inputs independently.

Processing of multiple signals at the same time could enable synthetic tissues to adjust to the patients' needs in real time and enable augmentation or replacement of native tissues in the human body.

References

ADAMS, G.B., MARTIN, R.P., ALLEY, I.R., CHABNER, K.T., COHEN, K.S., CALVI, L.M., KRONENBERG, H.M. and SCADDEN, D.T., 2007. Therapeutic targeting of a stem cell niche. Nature biotechnology, 25(2), pp. 238-243.

AIDELBERG, G., TOWBIN, B.D., ROTHSCHILD, D., DEKEL, E., BREN, A. and ALON, U., 2014. Hierarchy of non-glucose sugars in Escherichia coli. *BMC systems biology,* **8**(1), pp. 1-12.

ALCINESIO, A., MEACOCK, O.J., ALLAN, R.G., MONICO, C., SCHILD, V.R., CAZIMOGLU, I., CORNALL, M.T., KUMAR, R.K. and BAYLEY, H., 2020. Controlled packing and single-droplet resolution of 3D-printed functional synthetic tissues. *Nature communications,* **11**(1), pp. 1-13.

AMMAR, E.M., WANG, X. and RAO, C.V., 2018. Regulation of metabolism in Escherichia coli during growth on mixtures of the non-glucose sugars: arabinose, lactose, and xylose. *Scientific reports,* **8**(1), pp. 1-11.

AVEDISSIAN, S.N., LIU, J., RHODES, N.J., LEE, A., PAIS, G.M., HAUSER, A.R. and SCHEETZ, M.H., 2019. A review of the clinical pharmacokinetics of polymyxin B. *Antibiotics,* **8**(1), pp. 31.

BARLOW, N., SMPOKOU, E., FRIDDIN, M., MACEY, R., GOULD, I., TURNBULL, C., FLEMMING, A., BROOKS, N., CES, O. and BARTER, L., 2017. Engineering plant membranes using droplet interface bilayers. *Biomicrofluidics,* **11**(2), pp. 024107.

BAYLEY, H., CRONIN, B., HERON, A., HOLDEN, M.A., HWANG, W.L., SYEDA, R., THOMPSON, J. and WALLACE, M., 2008. Droplet interface bilayers. *Molecular BioSystems,* **4**(12), pp. 1191-1208.

BOOTH, M.J., SCHILD, V.R., BOX, S.J. and BAYLEY, H., 2017. Light-patterning of synthetic tissues with single droplet resolution. *Scientific reports,* **7**(1), pp. 1-10.

BOOTH, M.J., SCHILD, V.R., DOWNS, F.G. and BAYLEY, H., 2017. Functional aqueous droplet networks. *Molecular BioSystems,* **13**(9), pp. 1658-1691.

BOOTH, M.J., SCHILD, V.R., GRAHAM, A.D., OLOF, S.N. and BAYLEY, H., 2016. Light-activated communication in synthetic tissues. *Science Advances,* **2**(4), pp. e1600056.

DESAI, T.A. and RAO, C.V., 2010. Regulation of arabinose and xylose metabolism in Escherichia coli. *Applied and Environmental Microbiology,* **76**(5), pp. 1524-1532.

DUPIN, A. and SIMMEL, F.C., 2019. Signalling and differentiation in emulsion-based multi-compartmentalized in vitro gene circuits. *Nature chemistry,* **11**(1), pp. 32-39.

ELANI, Y., 2020. Interfacing living and synthetic cells as an emerging frontier in synthetic biology. *Angewandte Chemie International Edition,* .

ELANI, Y., LAW, R.V. and CES, O., 2014. Vesicle-based artificial cells as chemical microreactors with spatially segregated reaction pathways. *Nature communications,* **5**(1), pp. 1-5.

FROGER, A. and HALL, J.E., 2007. Transformation of plasmid DNA into E. coli using the heat shock method. *Journal of visualized experiments : JoVE,* **(6):253. doi**(6), pp. 253.

GARDNER, P.M., WINZER, K. and DAVIS, B.G., 2009. Sugar synthesis in a protocellular model leads to a cell signalling response in bacteria. *Nature chemistry,* **1**(5), pp. 377-383.

HOLDEN, M.A., NEEDHAM, D. and BAYLEY, H., 2007. Functional bionetworks from nanoliter water droplets. *Journal of the American Chemical Society,* **129**(27), pp. 8650-8655.

HUANG, S., ROMERO-RUIZ, M., CASTELL, O.K., BAYLEY, H. and WALLACE, M.I., 2015. High-throughput optical sensing of nucleic acids in a nanopore array. *Nature nanotechnology,* **10**(11), pp. 986-991.

KHLEBNIKOV, A., RISA, Ø., SKAUG, T., CARRIER, T.A. and KEASLING, J., 2000. Regulatable arabinose-inducible gene expression system with consistent control in all cells of a culture. *Journal of Bacteriology,* **182**(24), pp. 7029-7034.

KUMAR, R.K., MEILLER-LEGRAND, T., ALCINESIO, A., GONZALEZ, D., MAVRIDOU, D.A., MEACOCK, O.J., SMITH, W.P., ZHOU, L., KIM, W. and PULCU, G.S., 2020. Droplet printing reveals the importance of micron-scale structure for bacterial ecology. *bioRxiv,* .

KWOK, R., 2010. Five hard truths for synthetic biology. *Nature News,* **463**(7279), pp. 288-290.

LENTINI, R., MARTÍN, N.Y., FORLIN, M., BELMONTE, L., FONTANA, J., CORNELLA, M., MARTINI, L., TAMBURINI, S., BENTLEY, W.E., JOUSSON, O. and MANSY, S.S., 2017. Two-way chemical communication between artificial and natural cells. *ACS central science,* **3**(2), pp. 117-123.

LENTINI, R., SANTERO, S.P., CHIZZOLINI, F., CECCHI, D., FONTANA, J., MARCHIORETTO, M., DEL BIANCO, C., TERRELL, J.L., SPENCER, A.C., MARTINI, L. and MANSY, S.S., 2014. Integrating artificial with natural cells to translate chemical messages that direct E. coli behaviour. *Nature communications,* **5**(1), pp. 1-6.

LEPTIHN, S., CASTELL, O.K., CRONIN, B., LEE, E., GROSS, L.C., MARSHALL, D.P., THOMPSON, J.R., HOLDEN, M. and WALLACE, M.I., 2013. Constructing droplet interface bilayers from the contact of aqueous droplets in oil. *Nature protocols,* **8**(6), pp. 1048-1057.

LIU, S., QIN, S., HE, M., ZHOU, D., QIN, Q. and WANG, H., 2020. Current applications of poly (lactic acid) composites in tissue engineering and drug delivery. *Composites Part B: Engineering,* , pp. 108238.

MAI, Y. and EISENBERG, A., 2012. Self-assembly of block copolymers. *Chemical Society Reviews,* **41**(18), pp. 5969-5985.

PASTAR, I., STOJADINOVIC, O., YIN, N.C., RAMIREZ, H., NUSBAUM, A.G., SAWAYA, A., PATEL, S.B., KHALID, L., ISSEROFF, R.R. and TOMIC-CANIC, M., 2014. Epithelialization in wound healing: a comprehensive review. *Advances in wound care,* **3**(7), pp. 445-464.

RAMPIONI, G., D'ANGELO, F., MESSINA, M., ZENNARO, A., KURUMA, Y., TOFANI, D., LEONI, L. and STANO, P., 2018. Synthetic cells produce a quorum

sensing chemical signal perceived by Pseudomonas aeruginosa. *Chemical communications,* **54**(17), pp. 2090-2093.

SAGHAZADEH, S., RINOLDI, C., SCHOT, M., KASHAF, S.S., SHARIFI, F., JALILIAN, E., NUUTILA, K., GIATSIDIS, G., MOSTAFALU, P. and DERAKHSHANDEH, H., 2018. Drug delivery systems and materials for wound healing applications. *Advanced Drug Delivery Reviews,* **127**, pp. 138-166.

SAMBROOK, J., FRITSCH, E.F. and MANIATIS, T., 1989. *Molecular cloning: a laboratory manual.* Cold spring harbor laboratory press.

SCHUTGENS, F. and CLEVERS, H., 2020. Human organoids: tools for understanding biology and treating diseases. *Annual Review of Pathology: Mechanisms of Disease,* **15**, pp. 211-234.

SCHWARZ-SCHILLING, M., AUFINGER, L., MÜCKL, A. and SIMMEL, F., 2016. Chemical communication between bacteria and cell-free gene expression systems *within linear chains of emulsion droplets. Integrative Biology, 8(4), pp. 564-570.*

SHVARTSMAN, S.Y. and BAKER, R.E., 2012. Mathematical models of morphogen gradients and their effects on gene expression. Wiley Interdisciplinary Reviews: Developmental Biology, 1(5), pp. 715-730.

TOPARLAK, Ö.D., ZASSO, J., BRIDI, S., DALLA SERRA, M., MACCHI, P., CONTI, L., BAUDET, M. and MANSY, S.S., 2020. Artificial cells drive neural differentiation. *Science advances,* **6**(38), pp. eabb4920.

VILLAR, G., GRAHAM, A.D. and BAYLEY, H., 2013. A tissue-like printed material. Science, 340(6128), pp. 48-52.

WATSON, H., 2015. Biological membranes. Essays in biochemistry, 59, pp. 43-69.

YASUGA, H., KAWANO, R., TAKINOUE, M., TSUJI, Y., OSAKI, T., KAMIYA, K., MIKI, N. and TAKEUCHI, S., 2016. Logic gate operation by DNA translocation through biological nanopores. *PLoS One,* **11**(2), pp. e0149667.

ZHOU, L., WOLFES, A.C., LI, Y., CHAN, D.C., KO, H., SZELE, F.G. and BAYLEY, H., 2020. Lipid-bilayer-supported 3D printing of human cerebral cortex cells reveals developmental interactions. *Advanced Materials,* **32**(31), pp. 2002183.

The diagrams in this thesis were created using BioRender.com.